Observation of Rapid Frequency Chirping Instabilities Driven by Runaway Electrons in DIII-D

A. Lvovskiy[1]
with participation of
W.W. Heidbrink[2], C. Paz-Soldan[3], D.A. Spong[4], P. Aleynikov[5], A. Dal Molin[6], N.W. Eidietis[3], C. Liu[7], M. Nocente[6], D. Shiraki[4], L. Stagner[8], K.E. Thome[3], L. Giacomelli[9], D. Rigamonti[9], M. Tardocchi[9]

[1]Oak Ridge Associated Universities, Oak Ridge, TN, USA
[2]University of California, Irvine, Irvine, CA, USA
[3]General Atomics, San Diego, CA, USA
[4]Oak Ridge National Laboratory, Oak Ridge, TN, USA
[5]Max-Planck-Institut für Plasmaphysik, Greifswald, Germany
[6]Università di Milano-Bicocca, Milan, Italy
[7]Princeton Plasma Physics Laboratory, Princeton, NJ, USA
[8]Oak Ridge Institute for Science and Education, Oak Ridge, TN, USA
[9]Institute for Plasma Science and Technology, CNR, Milan, Italy

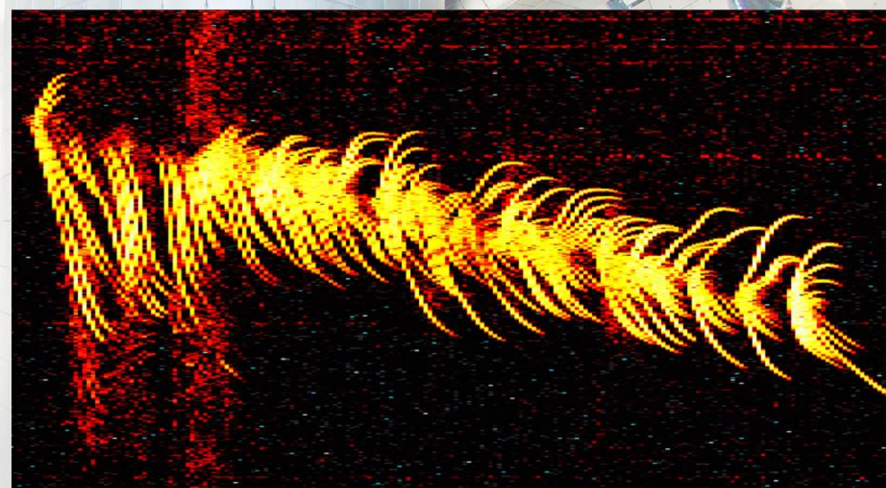

16th IAEA Technical Meeting on Energetic Particles
Shizuoka City, Japan
September 4, 2019

DIII-D NATIONAL FUSION FACILITY SAN DIEGO

ORAU

Frequency chirping instabilities are observed for the first time driven by runaway electrons in tokamak

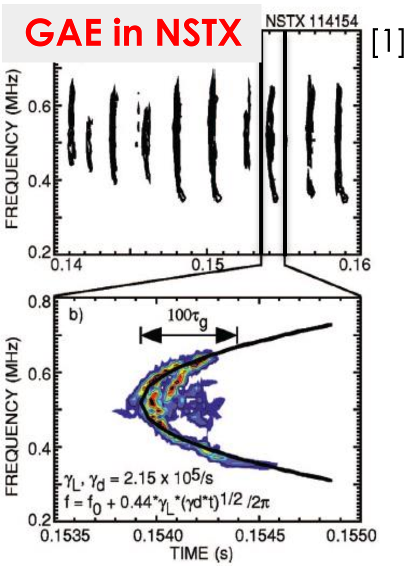

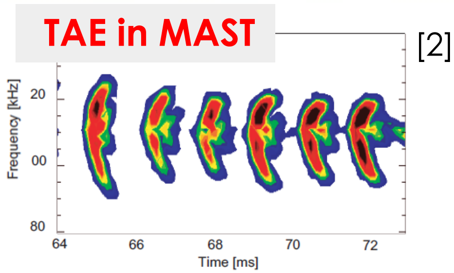

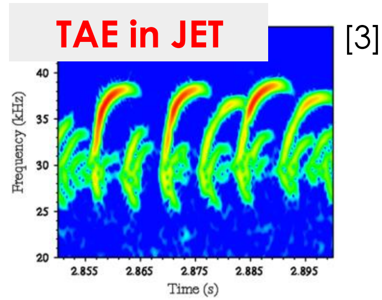

- **Energetic particles can drive instabilities through wave-particle resonances**
- **Frequency chirping instabilities are often observed driven by fast ions in tokamaks**

[1] Fredrickson *et al.* PoP 2006
[2] Pinches *et al.* PPCF 2004
[3] Berk *et al.* NF 2006

Frequency chirping instabilities are observed for the first time driven by runaway electrons in tokamak

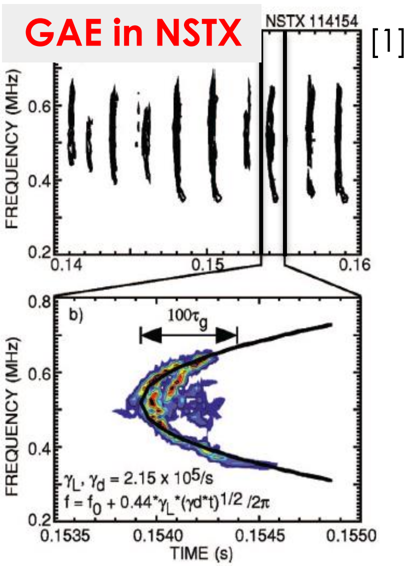

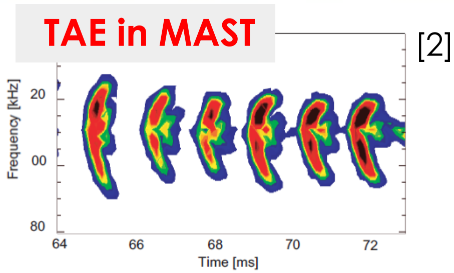

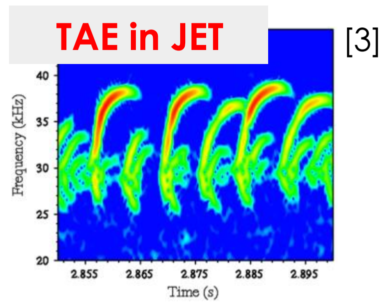

- Energetic particles can drive instabilities through wave-particle resonances
- Frequency chirping instabilities are often observed driven by fast ions in tokamaks
- **This talk: discovery of rapid frequency chirping driven by runaway electrons (REs) in DIII-D**

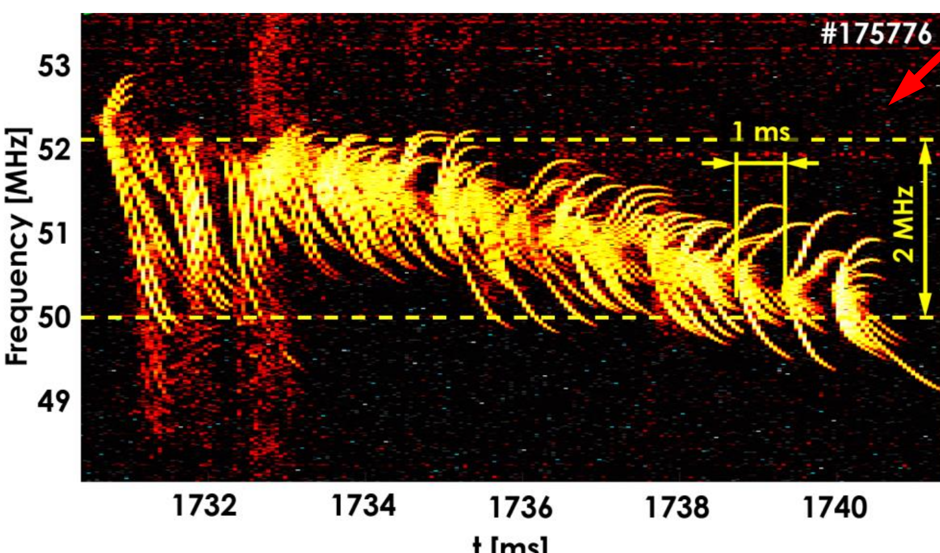

[1] Fredrickson *et al.* PoP 2006
[2] Pinches *et al.* PPCF 2004
[3] Berk *et al.* NF 2006

Frequency chirping instabilities are observed for the first time driven by runaway electrons in tokamak

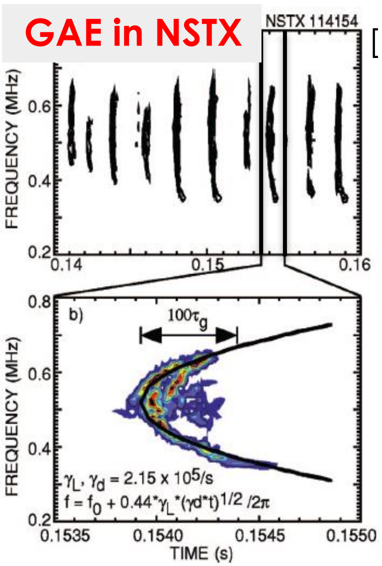

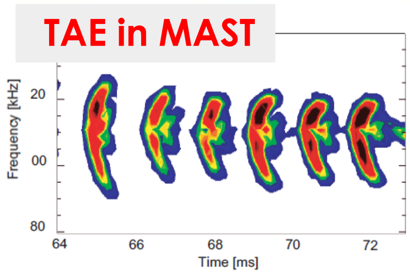

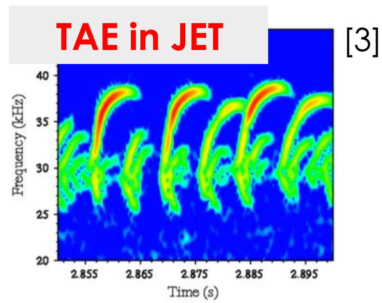

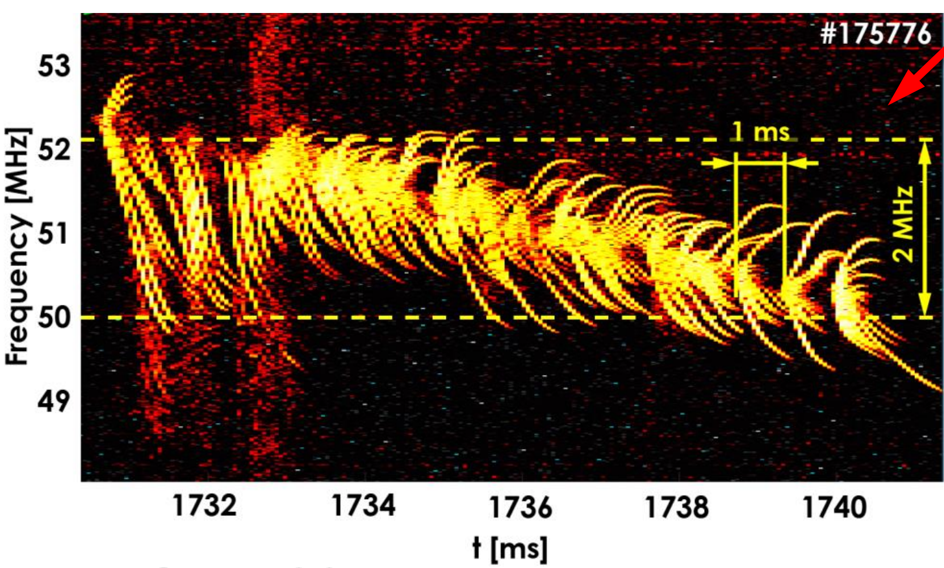

- **Energetic particles can drive instabilities through wave-particle resonances**
- **Frequency chirping instabilities are often observed driven by fast ions in tokamaks**
- **This talk: discovery of rapid frequency chirping driven by runaway electrons (REs) in DIII-D**
- **MHz instabilities increase RE loss**
- **While poorer confinement is undesirable for fast ions, it can be beneficial for RE control and mitigation in tokamaks**

[1] Fredrickson *et al.* PoP 2006
[2] Pinches *et al.* PPCF 2004
[3] Berk *et al.* NF 2006

Outline

- Experiment and diagnostics
- Frequency chirping
- RE distribution function
- Operating space
- Possible driving mechanism and candidate instability
- RE-driven instabilities at higher collisionality

Outline

- Experiment and diagnostics
- Frequency chirping
- RE distribution function
- Operating space
- Possible driving mechanism and candidate instability
- RE-driven instabilities at higher collisionality

RE-driven instabilities are accessed in low density post-disruption runaway plasma under decelerating voltage

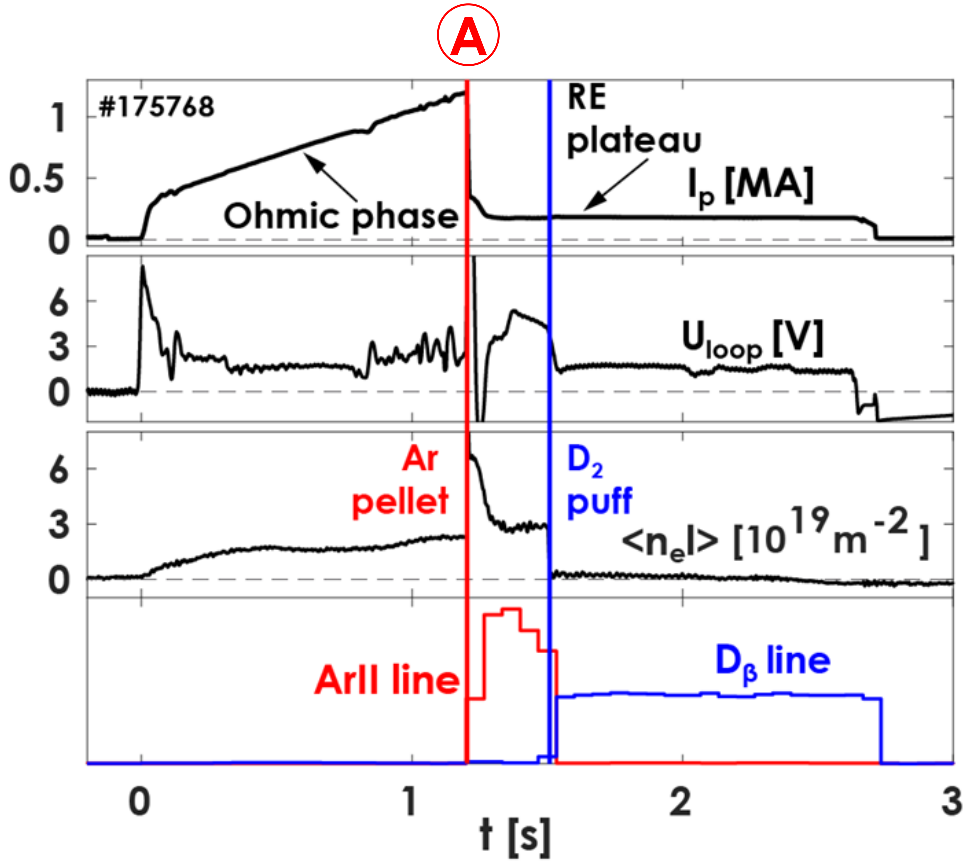

Ⓐ **Post-disruption RE beam is deliberately produced in DIII-D after injection of small Ar pellet**

RE-driven instabilities are accessed in low density post-disruption runaway plasma under decelerating voltage

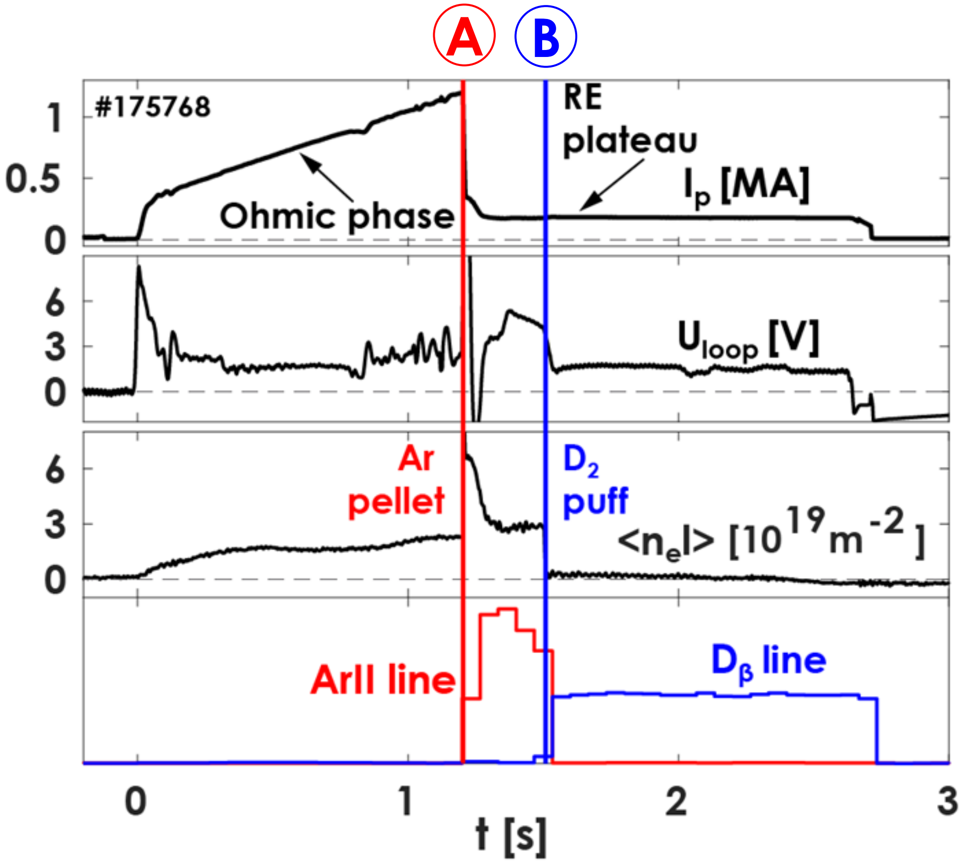

Ⓐ **Post-disruption RE beam is deliberately produced in DIII-D after injection of small Ar pellet**

Ⓑ **Argon impurity is purged from RE beam by D_2 massive gas injection**

- **This 1) drastically reduces thermal electron density by two orders of magnitude and 2) provides large variability of applied loop voltage**

DIII-D NATIONAL FUSION FACILITY SAN DIEGO

RE-driven instabilities are accessed in low density post-disruption runaway plasma under decelerating voltage

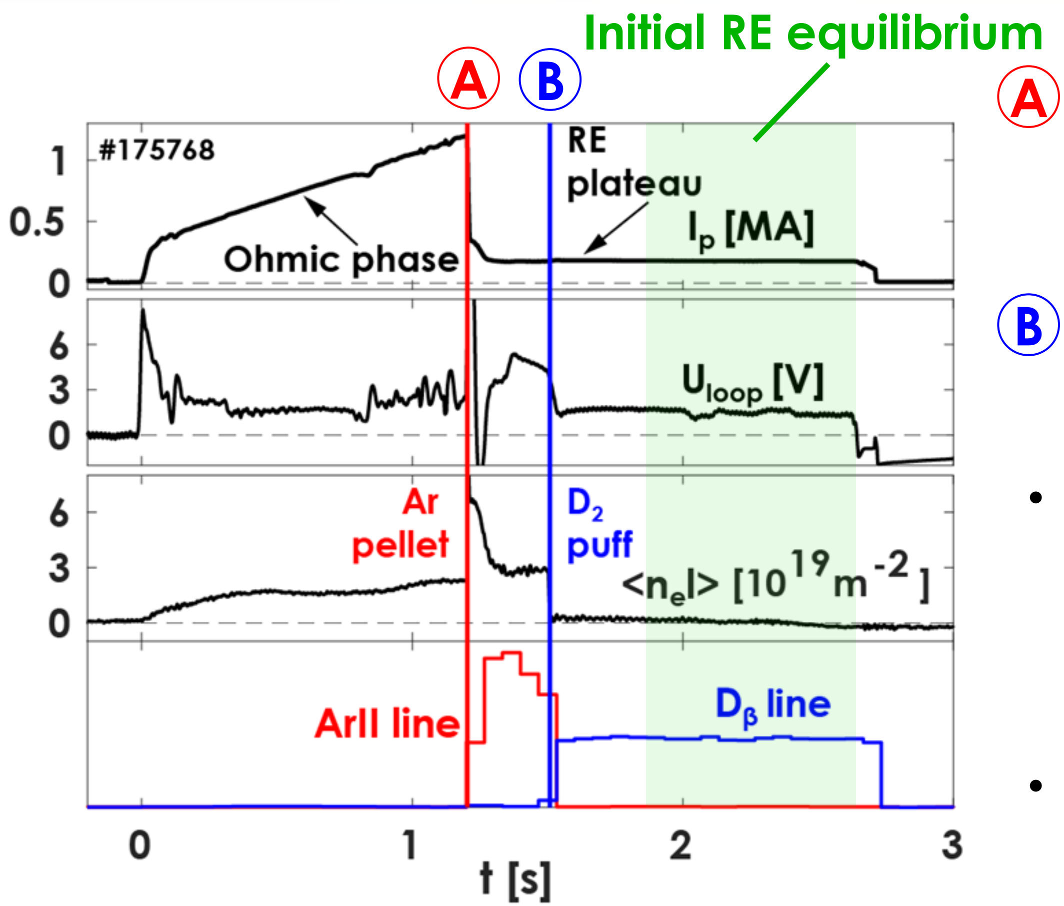

Ⓐ **Post-disruption RE beam is deliberately produced in DIII-D after injection of small Ar pellet**

Ⓑ **Argon impurity is purged from RE beam by D_2 massive gas injection**

- This 1) drastically reduces thermal electron density by two orders of magnitude and 2) provides large variability of applied loop voltage
- RE-driven instabilities are observed when large decelerating loop voltage is applied to initially stable RE beam (→ next slide)

DIII-D NATIONAL FUSION FACILITY SAN DIEGO

RE loss increases under decelerating loop voltage

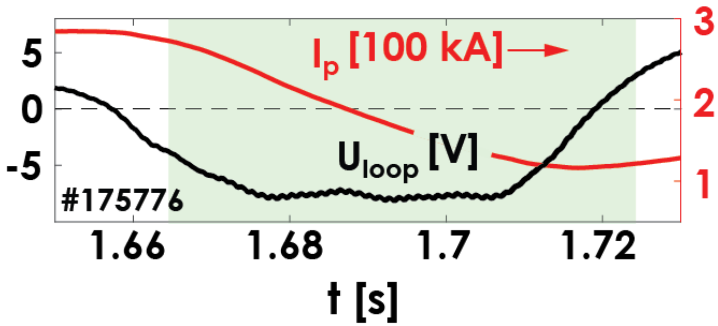

- **Large decelerating voltage with magnitude comparable with breakdown voltage is applied to RE beam**

DIII-D NATIONAL FUSION FACILITY SAN DIEGO

RE loss increases under decelerating loop voltage

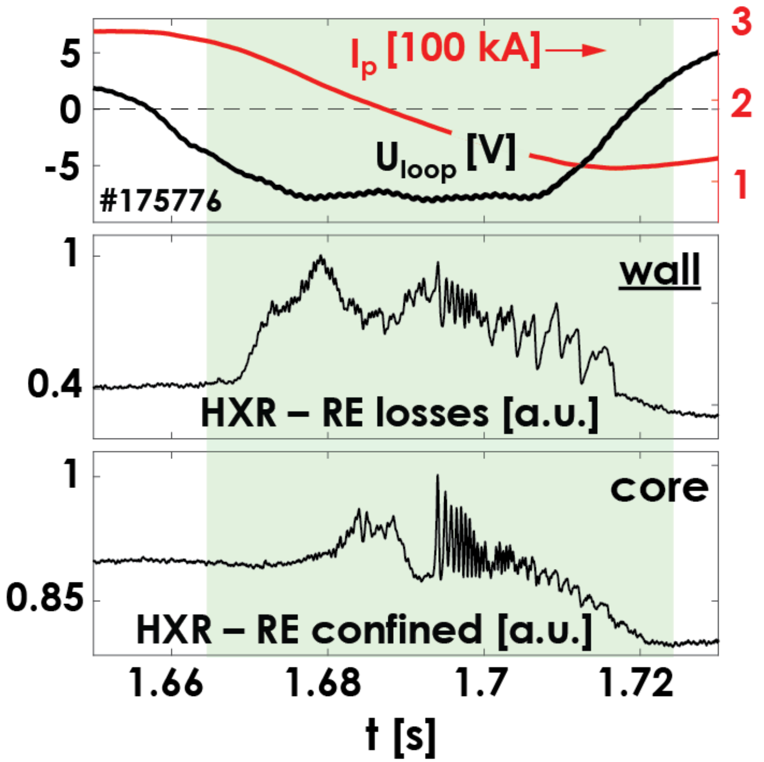

- **Large decelerating voltage with magnitude comparable with breakdown voltage is applied to RE beam**
- **This causes large fluctuations of wall and core hard X-ray signals (from lost and confined REs)**

RE loss increases under decelerating loop voltage

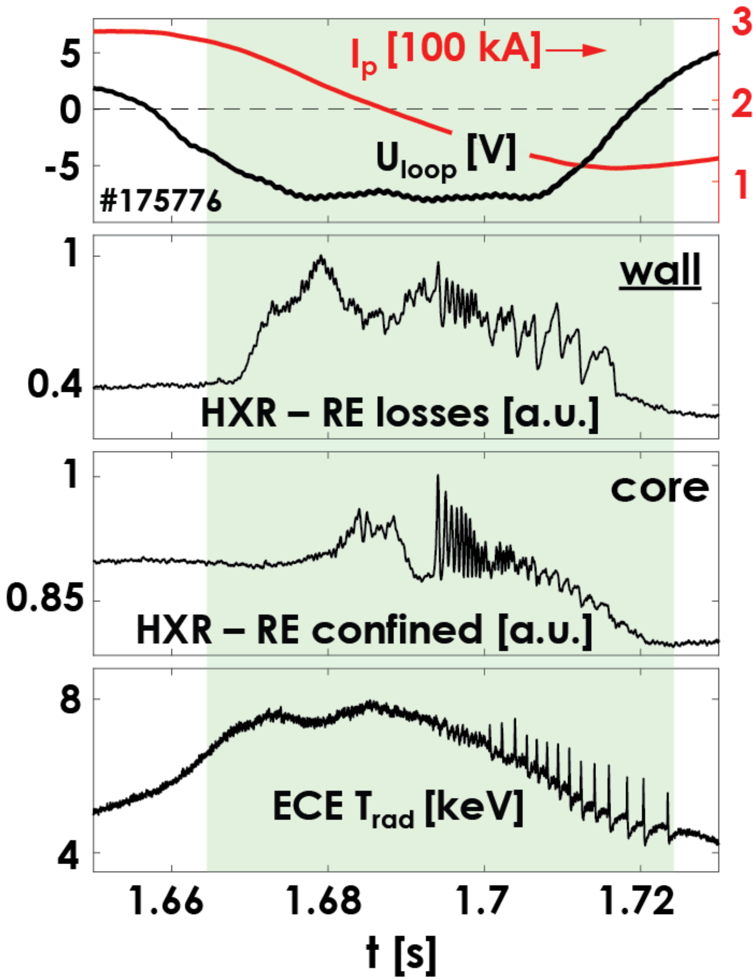

- **Large decelerating voltage with magnitude comparable with breakdown voltage is applied to RE beam**
- **This causes large fluctuations of wall and core hard X-ray signals (from lost and confined REs)**
- **Also, spikes of ECE are detected**

RE loss increases under decelerating loop voltage

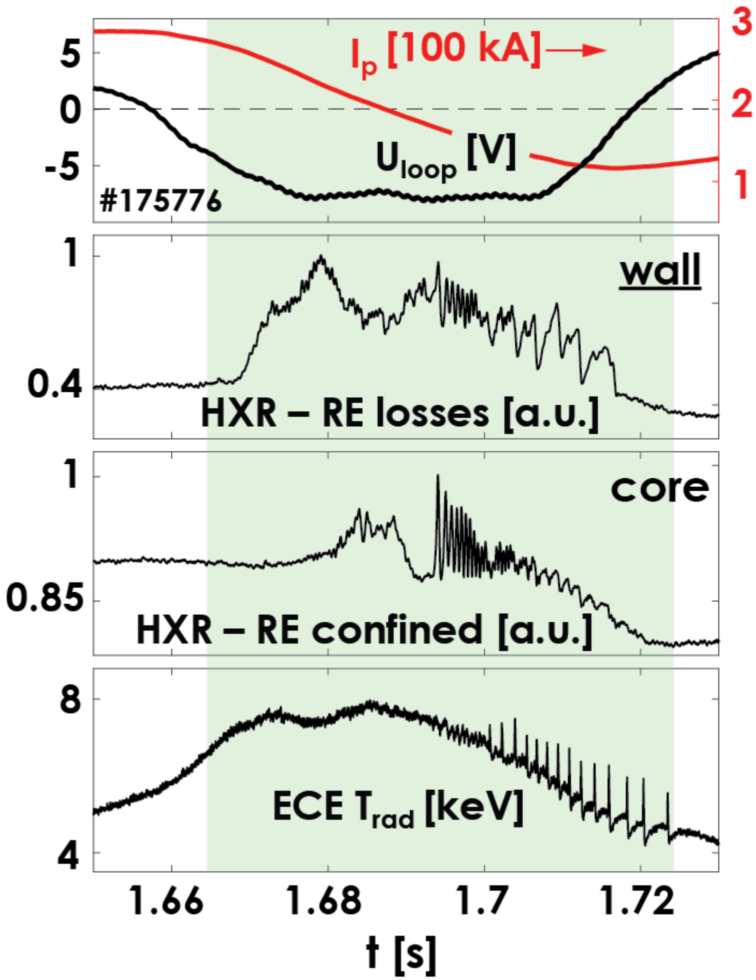

- Large decelerating voltage with magnitude comparable with breakdown voltage is applied to RE beam
- This causes large fluctuations of wall and core hard X-ray signals (from lost and confined REs)
- Also, spikes of ECE are detected
- These are clear signs of RE-driven instabilities

Outline

- Experiment and diagnostics
- Frequency chirping
- RE distribution function
- Operating space
- Possible driving mechanism and candidate instability
- RE-driven instabilities at higher collisionality

RE-driven plasma waves are detected via high-frequency measurements of magnetic signals

- **Energetic REs can lead to excitation of plasma waves *(similar to fast ions)***
- **High-frequency fluctuations of toroidal magnetic field are detected on DIII-D by RF-diagnostic [1,2]**
- **RF-diagnostic provides measurements up to 200 MHz**

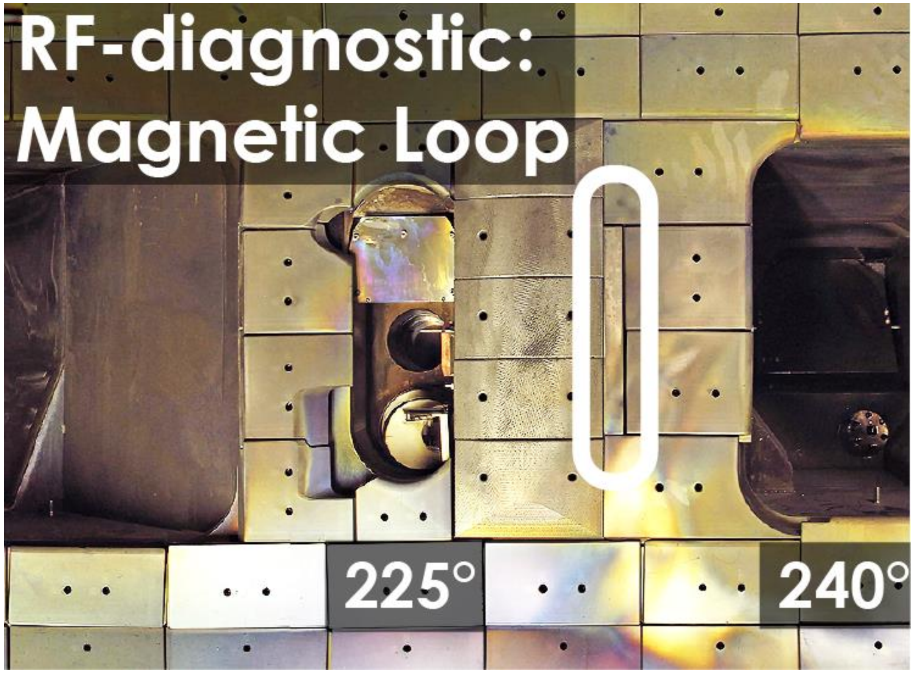

[1] Watson and Heidbrink RSI 2003
[2] Thome *et al*. RSI 2018

Bremsstrahlung radiation provides information on energy and distribution of REs

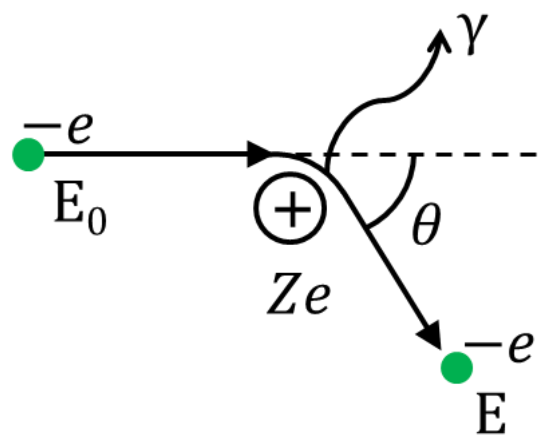

- **When electron changes its trajectory it emits photons**
- **MeV electrons → MeV γ rays**
- **γ rays (HXRs) are forward beamed based on RE energy**

Bremsstrahlung radiation provides information on energy and distribution of REs

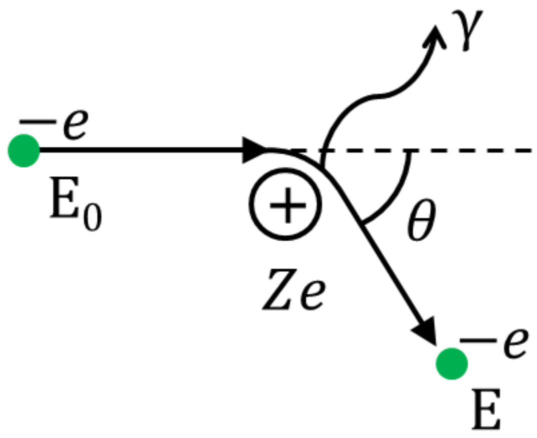

- When electron changes its trajectory it emits photons
- MeV electrons → MeV γ rays
- γ rays (HXRs) are forward beamed based on RE energy
- $f_e(E_{\parallel}, E_{\perp})$ produces unique bremsstrahlung spectrum

Bremsstrahlung radiation provides information on energy and distribution of REs

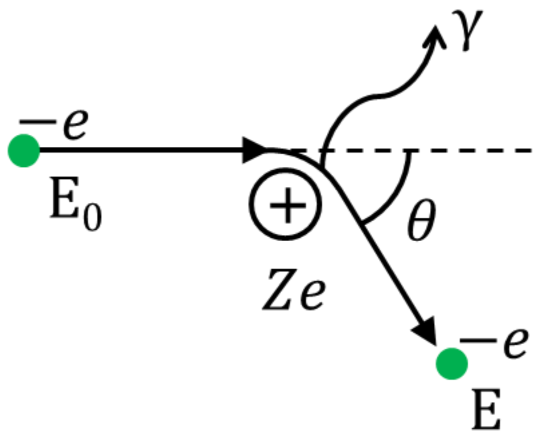

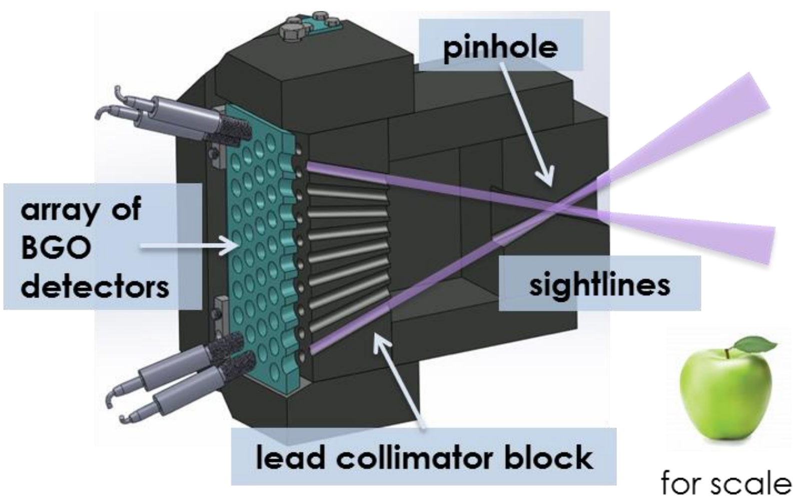

- **When electron changes its trajectory it emits photons**
- **MeV electrons → MeV γ rays**
- **γ rays (HXRs) are forward beamed based on RE energy**
- **$f_e(E_\parallel, E_\perp)$ produces unique bremsstrahlung spectrum**
- **DIII-D Gamma Ray Imager (GRI) provides 2D view of RE bremsstrahlung emission [1−4]**

[1] Pace *et al*. RSI 2016
[2] Cooper *et al*. RSI 2016
[3] Paz-Soldan *et al*. PRL 2017
[4] Paz-Soldan *et al*. PoP 2018

Bremsstrahlung radiation provides information on energy and distribution of REs

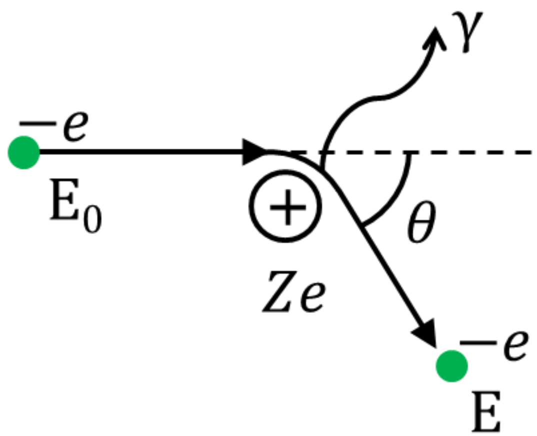

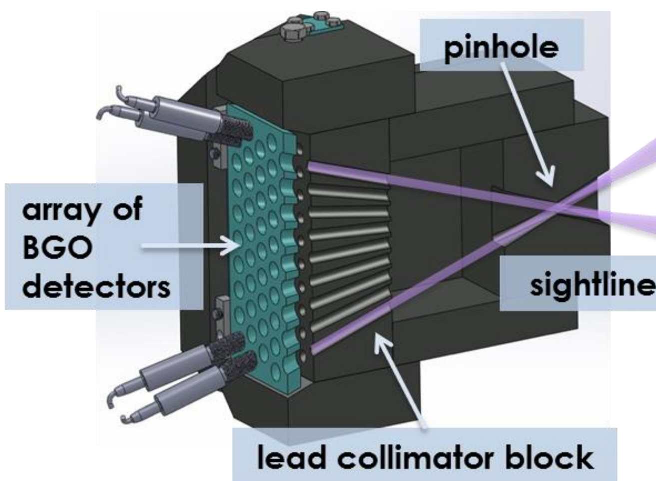


for scale

- When electron changes its trajectory it emits photons
- MeV electrons → MeV γ rays
- γ rays (HXRs) are forward beamed based on RE energy
- $f_e(E_{\parallel}, E_{\perp})$ produces unique bremsstrahlung spectrum
- DIII-D Gamma Ray Imager (GRI) provides 2D view of RE bremsstrahlung emission [1–4]

See also poster on RE orbit tomography by Luke Stagner on Thursday

[1] Pace *et al*. RSI 2016
[2] Cooper *et al*. RSI 2016
[3] Paz-Soldan *et al*. PRL 2017
[4] Paz-Soldan *et al*. PoP 2018

Outline

- Experiment and diagnostics
- Frequency chirping
- RE distribution function
- Operating space
- Possible driving mechanism and candidate instability
- RE-driven instabilities at higher collisionality

RE loss increases under decelerating loop voltage

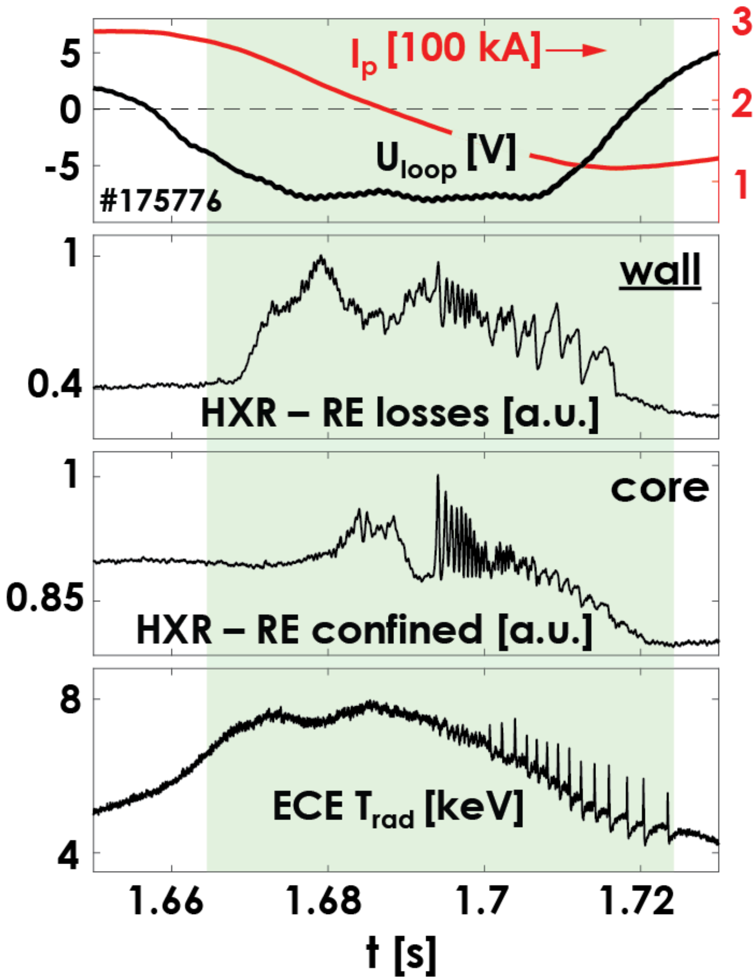

- Large decelerating voltage with magnitude comparable with breakdown voltage is applied to RE beam
- This causes large fluctuations of wall and core hard X-ray signals (from lost and confined REs)
- Also, spikes of ECE are detected
- These are clear signs of RE-driven instabilities
- Now take a close look at these instabilities

DIII-D NATIONAL FUSION FACILITY SAN DIEGO

RE loss correlates with magnetic fluctuations at 1–7 MHz

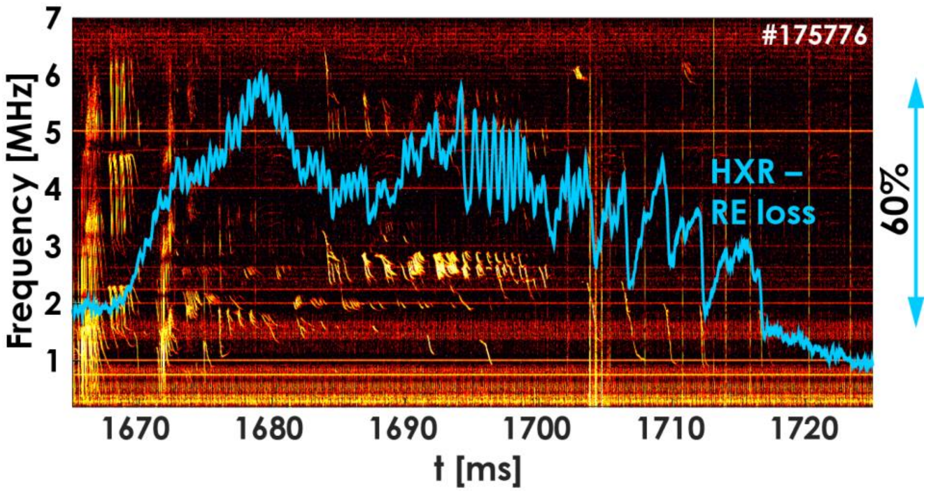

- **Fluctuations of toroidal magnetic field are seen in spectrograms**

RE loss correlates with magnetic fluctuations at 1–7 MHz

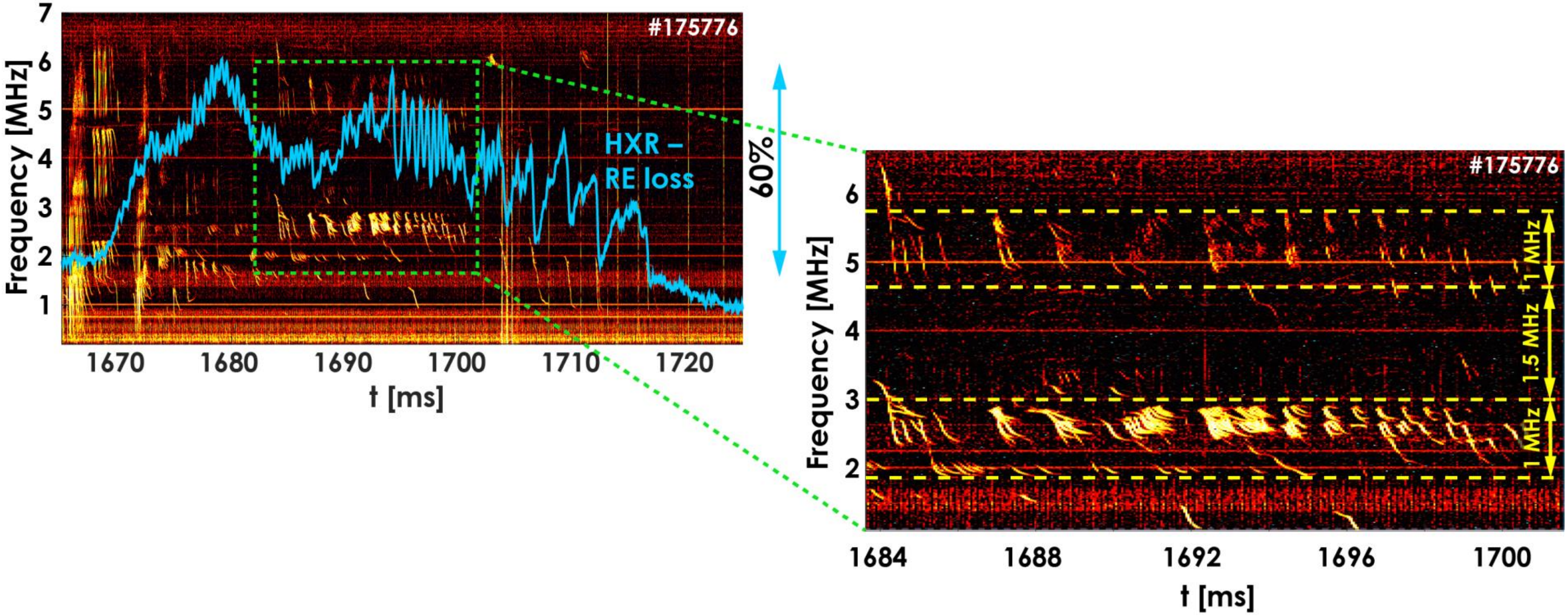

- Fluctuations of toroidal magnetic field are seen in spectrograms
- They have clear chirping nature

DIII-D NATIONAL FUSION FACILITY SAN DIEGO

RE loss correlates with magnetic fluctuations at 1–7 MHz

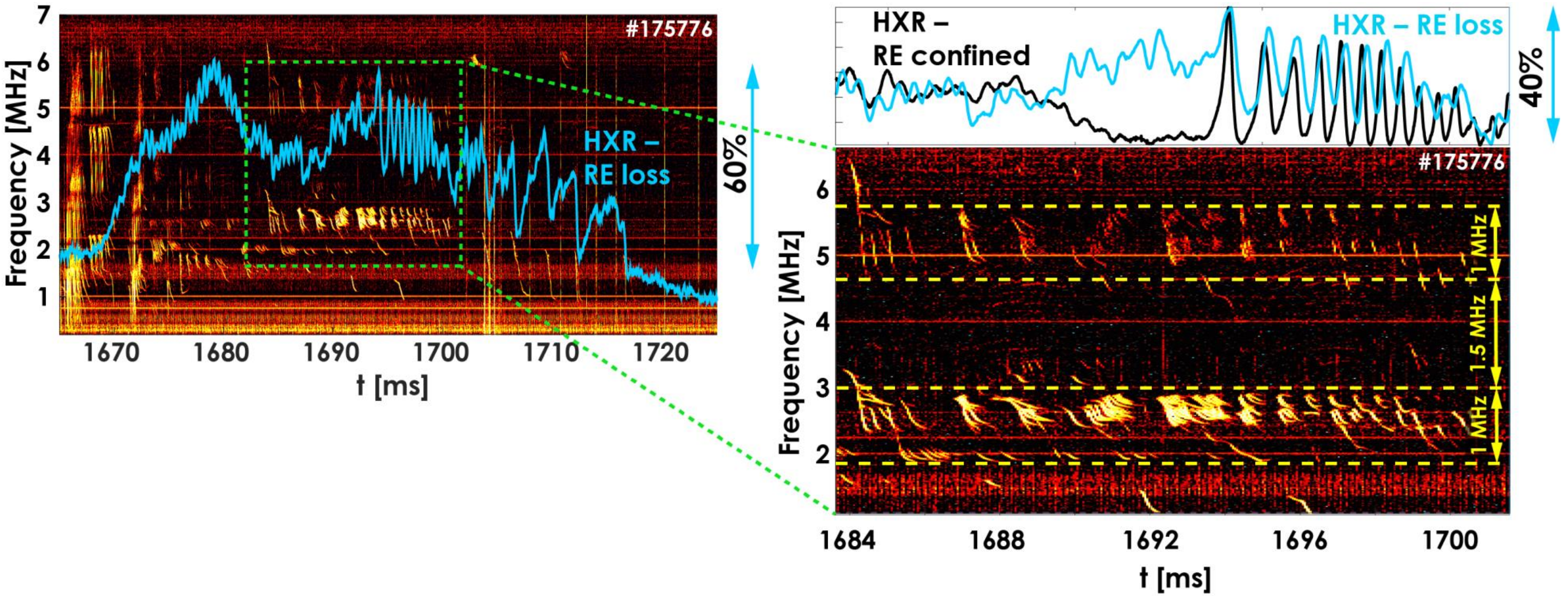

- Fluctuations of toroidal magnetic field are seen in spectrograms
- They have clear chirping nature and correlate with RE loss signal

DIII-D NATIONAL FUSION FACILITY SAN DIEGO

High frequency range magnetic fluctuations (30–80 MHz) show no correlation with RE loss

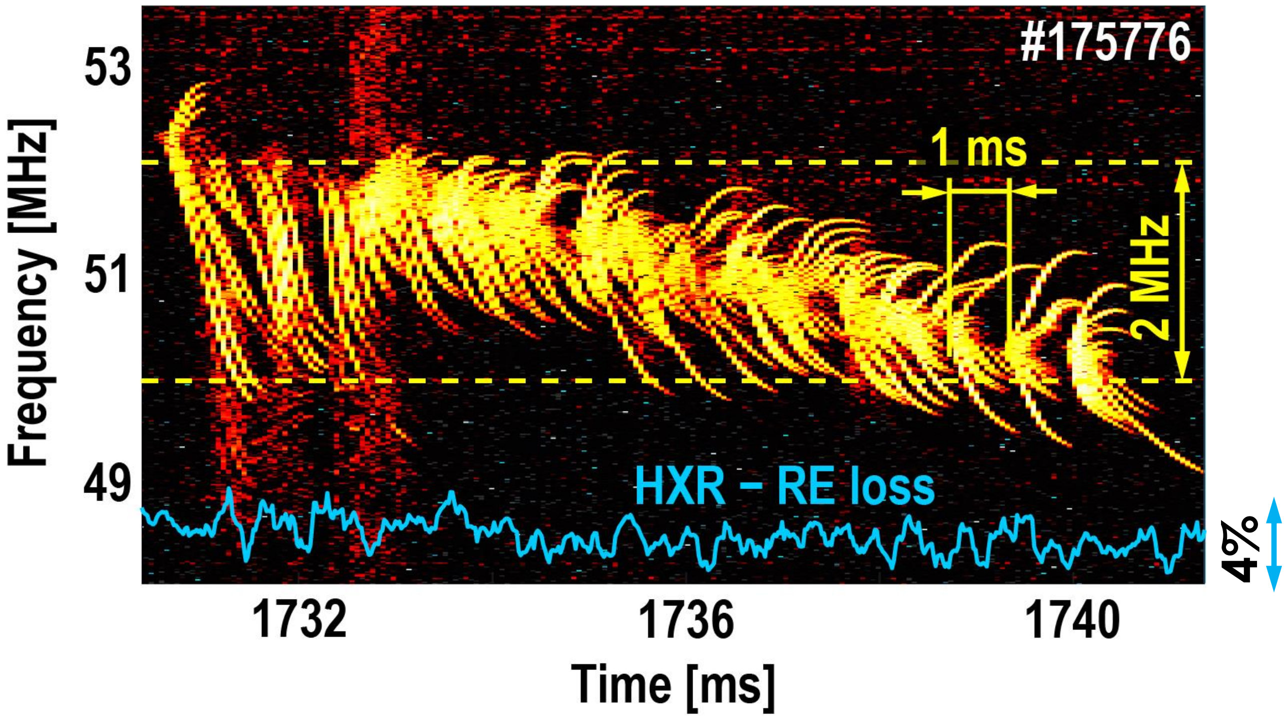

- Two frequency bands of magnetic fluctuations: 1–10 MHz and 30–80 MHz
- High frequency fluctuations do not drive observable RE loss

Frequency of instabilities has Alfvénic dependence on B_φ

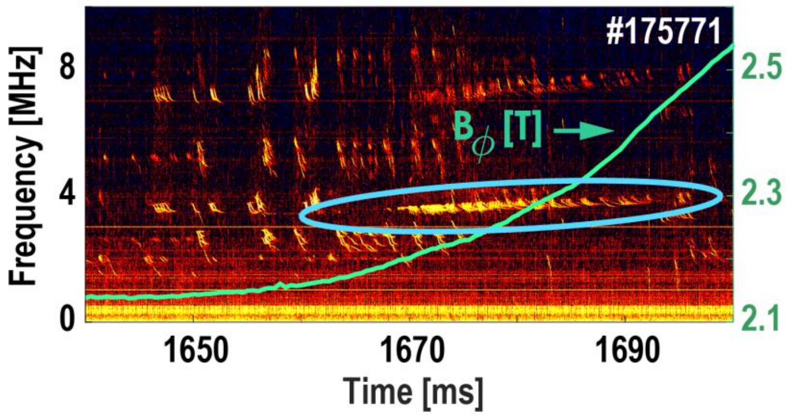

- RE beam moves to HFS and senses increasing $B_\varphi \propto 1/R$ (n_e=constant)

Frequency of instabilities has Alfvénic dependence on B_φ

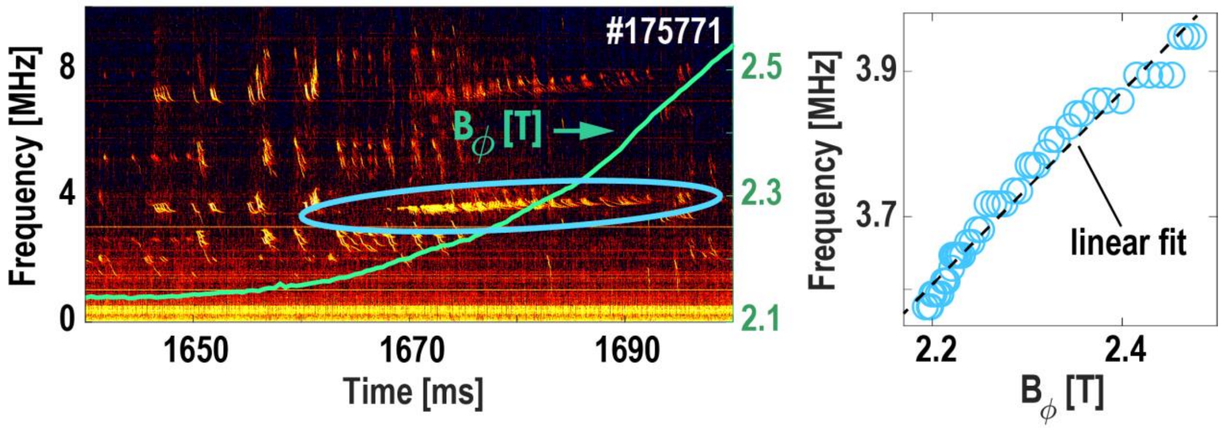

- **RE beam moves to HFS and senses increasing $B_\varphi \propto 1/R$ (n_e=constant)**
- **$f(B_\varphi)$ dependence is Alfvénic: $f_A \propto v_A \propto B_\varphi$**

Frequency of instabilities has Alfvénic dependence on B_φ

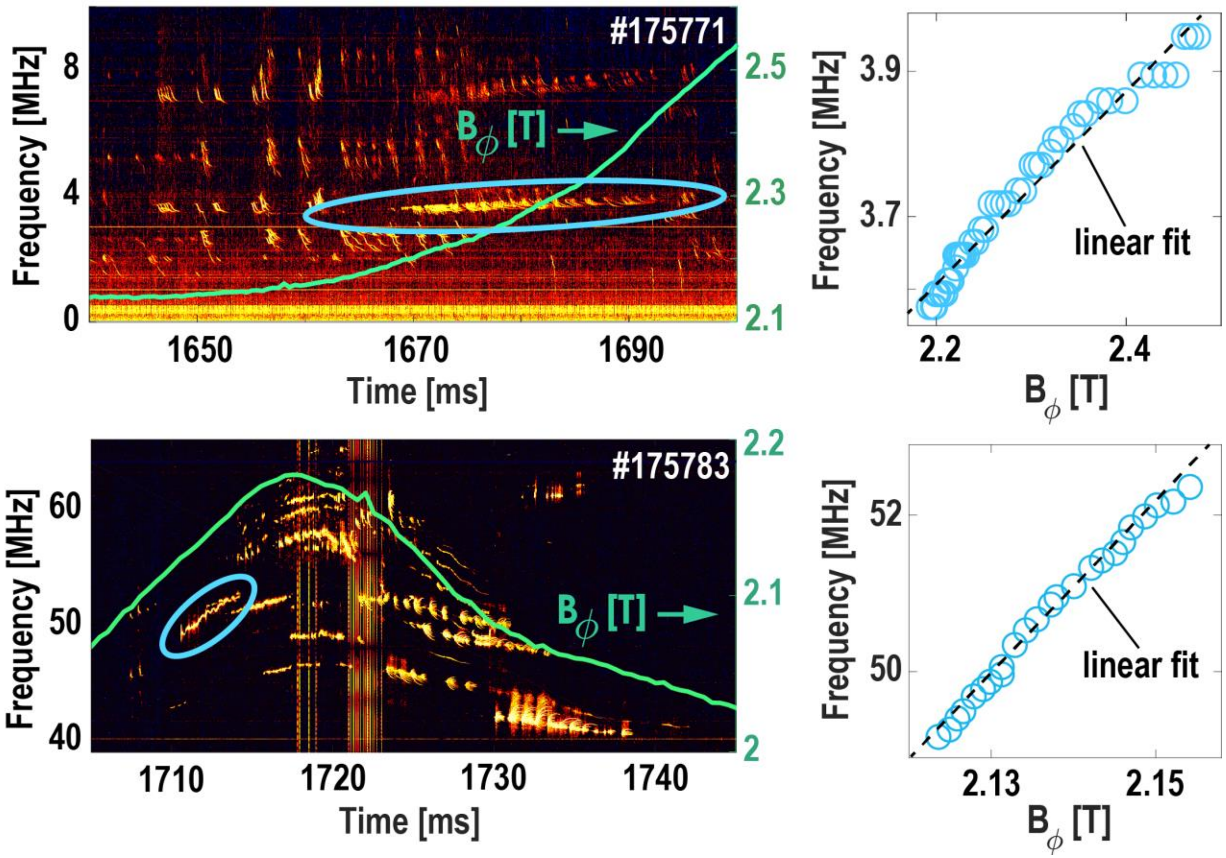

- RE beam moves to HFS and senses increasing $B_\varphi \propto 1/R$ (n_e=constant)
- $f(B_\varphi)$ dependence is Alfvénic: $f_A \propto v_A \propto B_\varphi$ for both frequency bands

DIII-D NATIONAL FUSION FACILITY SAN DIEGO

Outline

- Experiment and diagnostics
- Frequency chirping
- RE distribution function
- Operating space
- Possible driving mechanism and candidate instability
- RE-driven instabilities at higher collisionality

Modification of RE energy distribution function is measured during frequency chirping

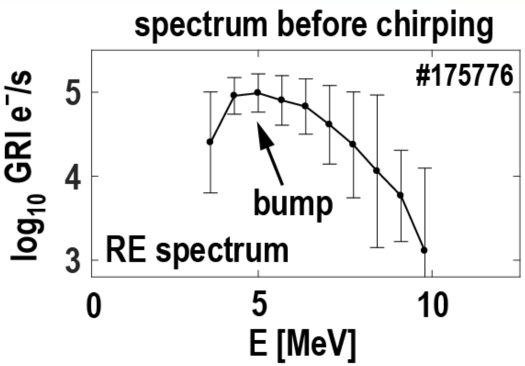

- **RE distribution function measured before chirping observed has a bump**

Modification of RE energy distribution function is measured during frequency chirping

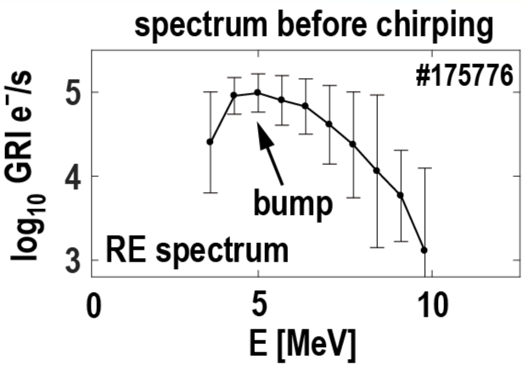

- **RE distribution function measured before chirping observed has a bump**
- **Bump is a potential source of free energy to drive instabilities**
- **Formation of the bump can be explained by interplay between RE acceleration by electric field and collisional damping on D_2 bound electrons [1]**

[1] Lvovskiy *et al*. *RE beam dynamics at low plasma density in DIII-D*. Submitted to Nucl. Fusion

Modification of RE energy distribution function is measured during frequency chirping

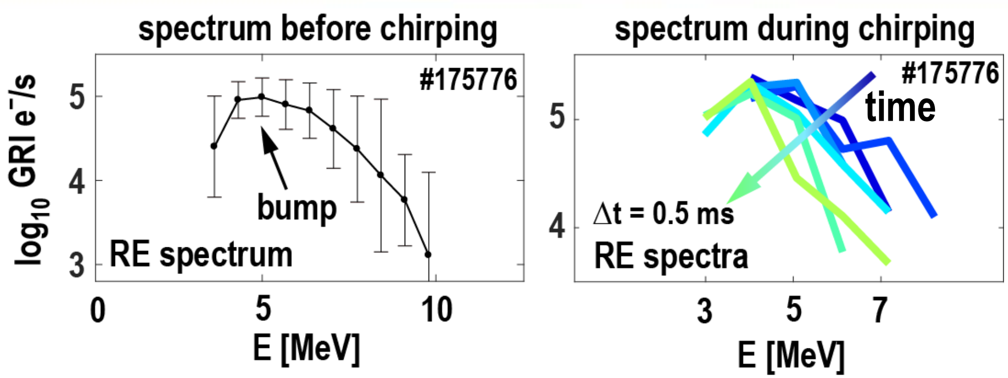

- RE distribution function measured before chirping observed has a bump
- Bump is a potential source of free energy to drive instabilities
- Formation of the bump can be explained by interplay between RE acceleration by electric field and collisional damping on D_2 bound electrons [1]
- Relaxation of RE f(E) during chirping events is directly measured

[1] Lvovskiy *et al*. *RE beam dynamics at low plasma density in DIII-D*. Submitted to Nucl. Fusion

Modification of RE energy distribution function is measured during frequency chirping

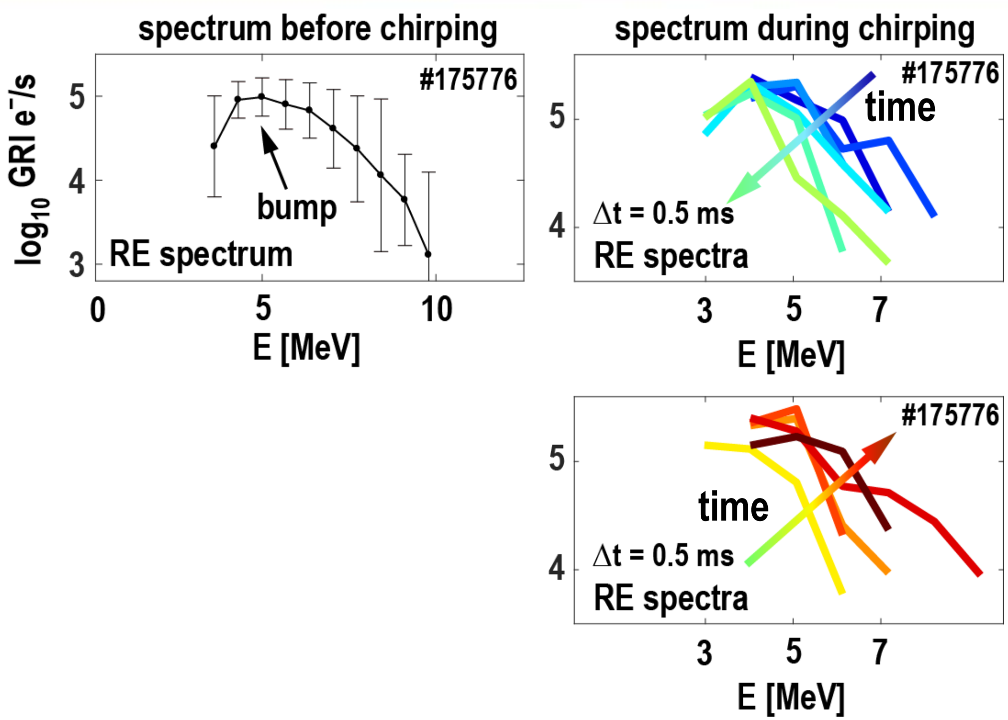

- **RE distribution function measured before chirping observed has a bump**
- **Bump is a potential source of free energy to drive instabilities**
- **Formation of the bump can be explained by interplay between RE acceleration by electric field and collisional damping on D_2 bound electrons [1]**
- **Relaxation of RE f(E) during chirping events is directly measured**

[1] Lvovskiy *et al*. *RE beam dynamics at low plasma density in DIII-D*. Submitted to Nucl. Fusion

Modification of RE energy distribution function is measured during frequency chirping

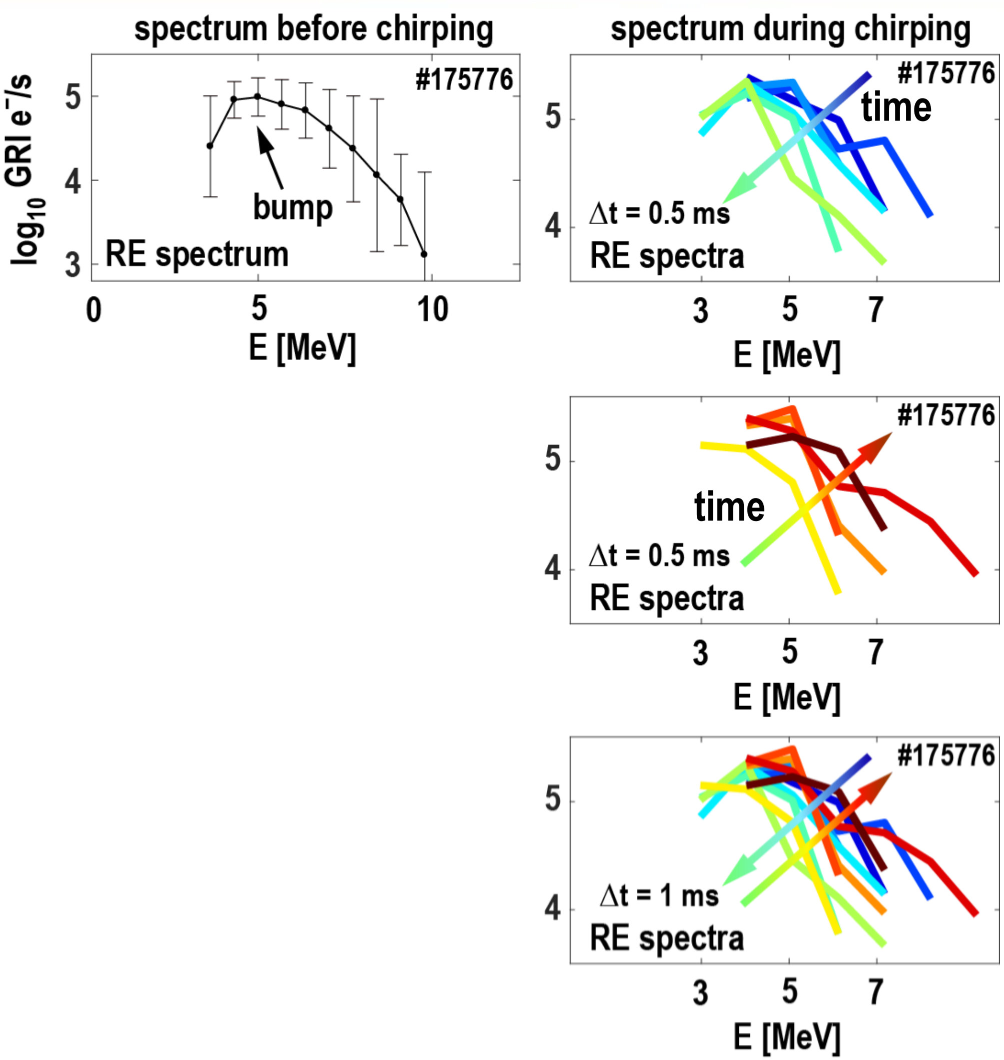

- **RE distribution function measured before chirping observed has a bump**
- **Bump is a potential source of free energy to drive instabilities**
- **Formation of the bump can be explained by interplay between RE acceleration by electric field and collisional damping on D_2 bound electrons [1]**
- **Relaxation of RE f(E) during chirping events is directly measured**

[1] Lvovskiy *et al. RE beam dynamics at low plasma density in DIII-D.* Submitted to Nucl. Fusion

Modification of RE energy distribution function is measured during frequency chirping

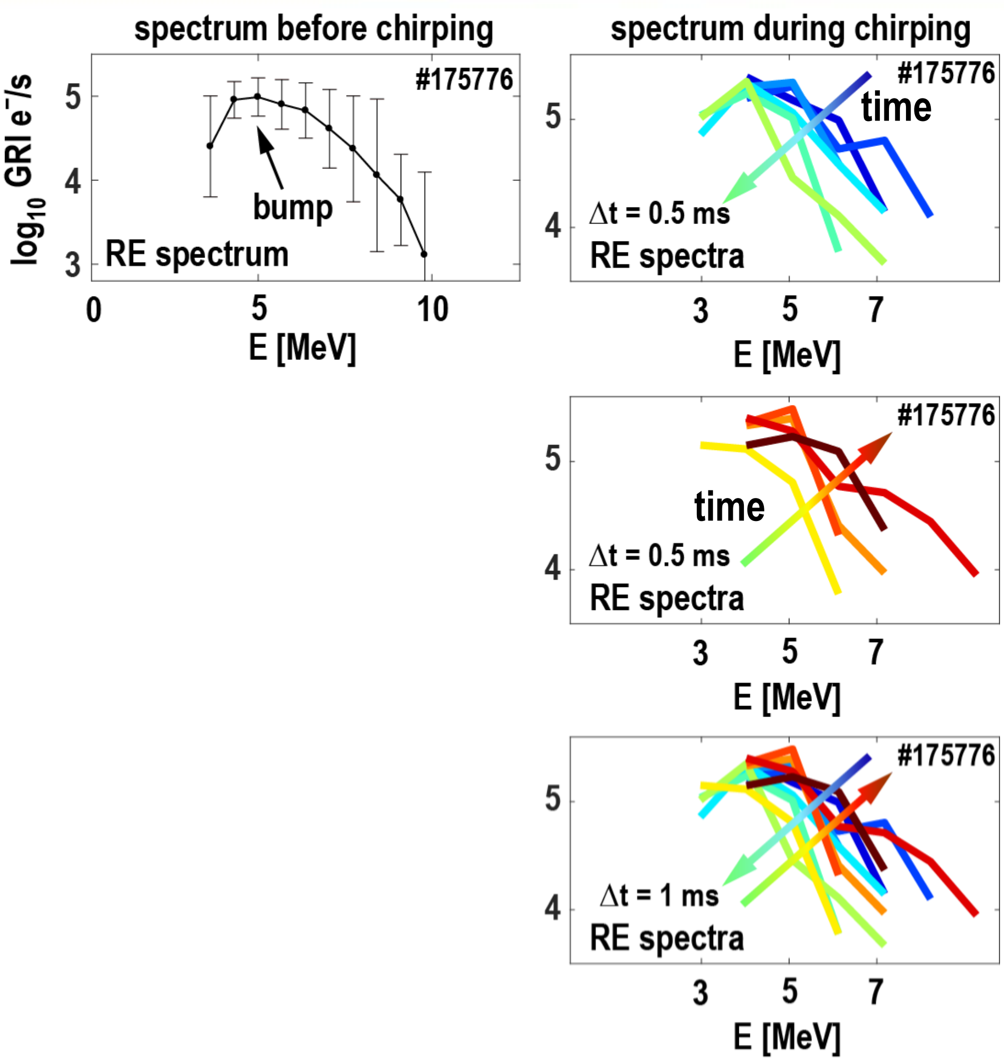

- **RE distribution function measured before chirping observed has a bump**
- **Bump is a potential source of free energy to drive instabilities**
- **Formation of the bump can be explained by interplay between RE acceleration by electric field and collisional damping on D_2 bound electrons [1]**
- **Relaxation of RE f(E) during chirping events is directly measured**
- **This supports interactions between REs and instabilities**

[1] Lvovskiy *et al. RE beam dynamics at low plasma density in DIII-D.* Submitted to Nucl. Fusion

Outline

- Experiment and diagnostics
- Frequency chirping
- RE distribution function
- Operating space
- Possible driving mechanism and candidate instability
- RE-driven instabilities at higher collisionality

Chirping in low frequency range causes strongest RE loss

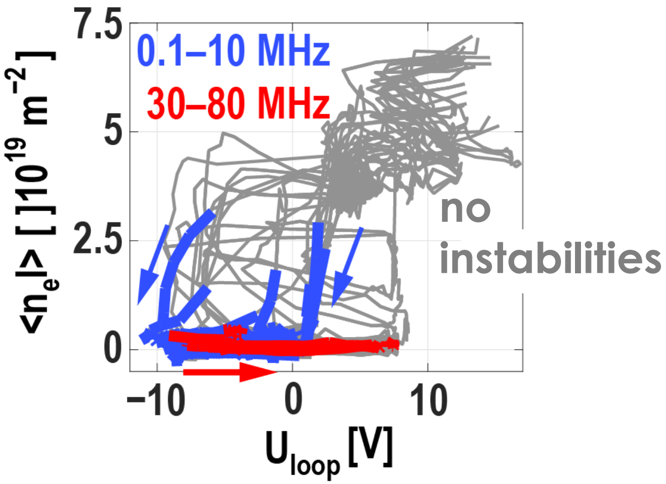

- Instabilities are observed in two distinct frequency ranges: 0.1−10 MHz and 30−80 MHz
- They are triggered at low plasma density and decelerating voltage

Chirping in low frequency range causes strongest RE loss

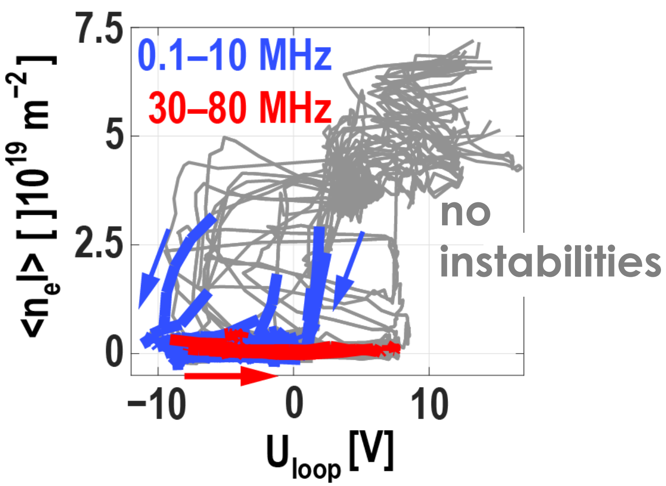

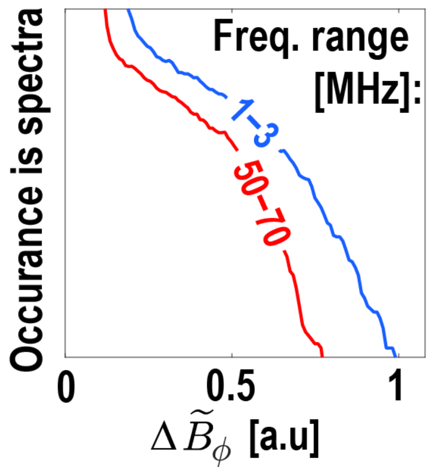

- Instabilities are observed in two distinct frequency ranges: 0.1−10 MHz and 30−80 MHz
- They are triggered at low plasma density and decelerating voltage
- Low freq. chirping (1−3 MHz) causes the strongest magnetic fluctuations ($\Delta\widetilde{B}_\phi$)

Chirping in low frequency range causes strongest RE loss

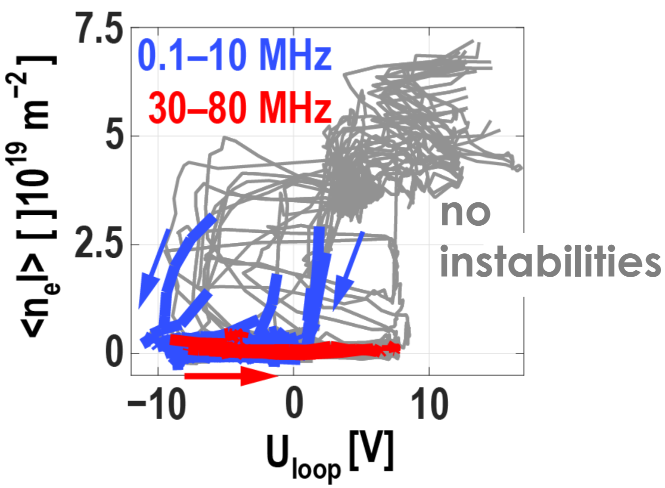

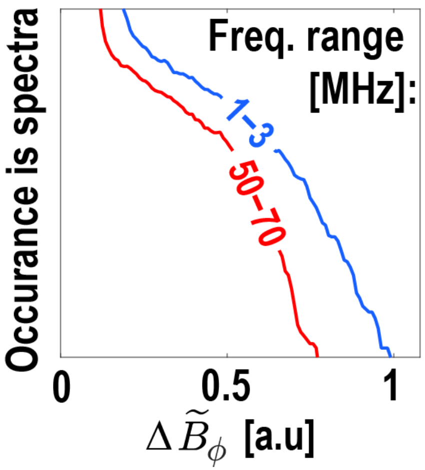

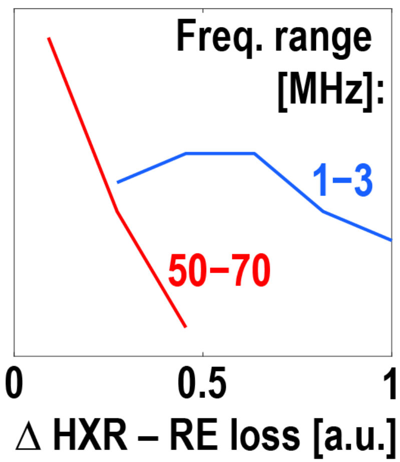

- Instabilities are observed in two distinct frequency ranges: 0.1−10 MHz and 30−80 MHz
- They are triggered at low plasma density and decelerating voltage
- Low freq. chirping (1−3 MHz) causes the strongest magnetic fluctuations ($\Delta\widetilde{B}_\phi$)
- Low freq. chirping (1−3 MHz) causes the strongest change of RE loss signal (ΔHXR)
- Δf changes by 0.3−2.4 MHz on 0.1 ms (local width) and 0.3-1.8 ms (full width) time scales

Outline

- Experiment and diagnostics
- Frequency chirping
- RE distribution function
- Operating space
- Possible driving mechanism and candidate instability
- RE-driven instabilities at higher collisionality

Possible mechanism of instabilities: REs drive Alfvénic waves, which scatter REs and increase RE loss

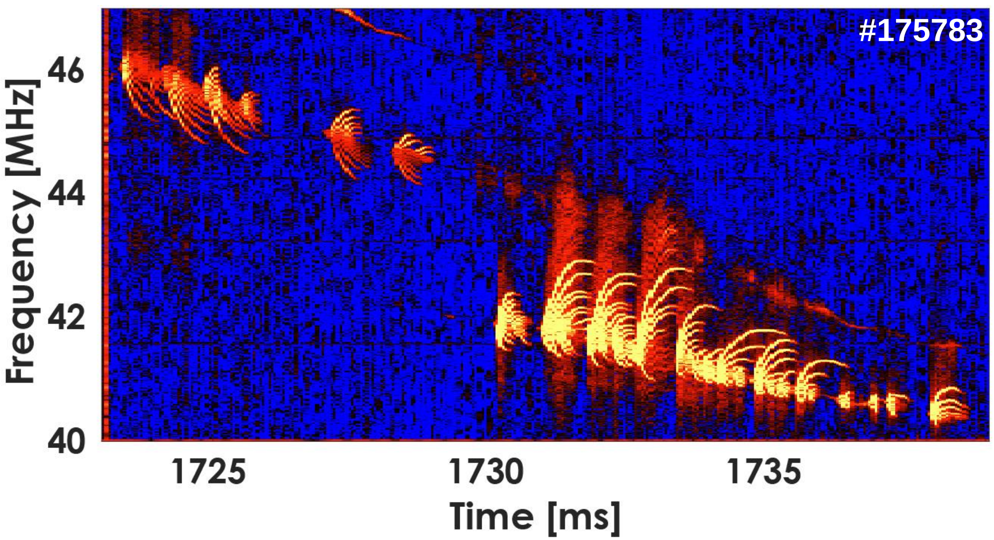

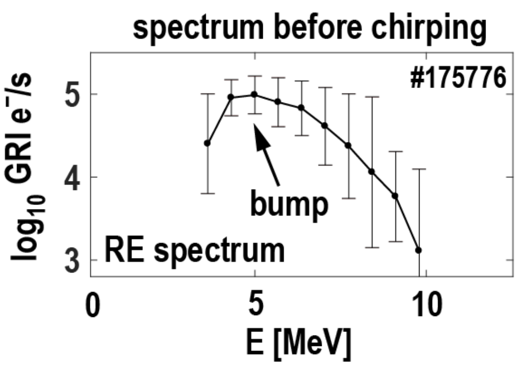

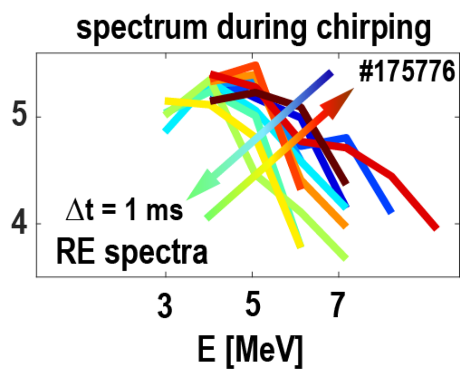

- Decelerating loop voltage presumably leads to strong non-monotonic feature (bump) at RE distribution function
- This excites Alfvénic waves
- Alfvénic waves interact with REs, scatter them and increase RE loss
- Fast relaxation of RE distribution function can explain frequency chirping consistent with the hole-clump model [1]
- Fast pitch-angle scattering of REs can cause the observed spikes of ECE

[1] Berk, Breizman, Ye. PRL 1992

Compressional Alfvén eigenmodes are most likely candidates for observed instabilities

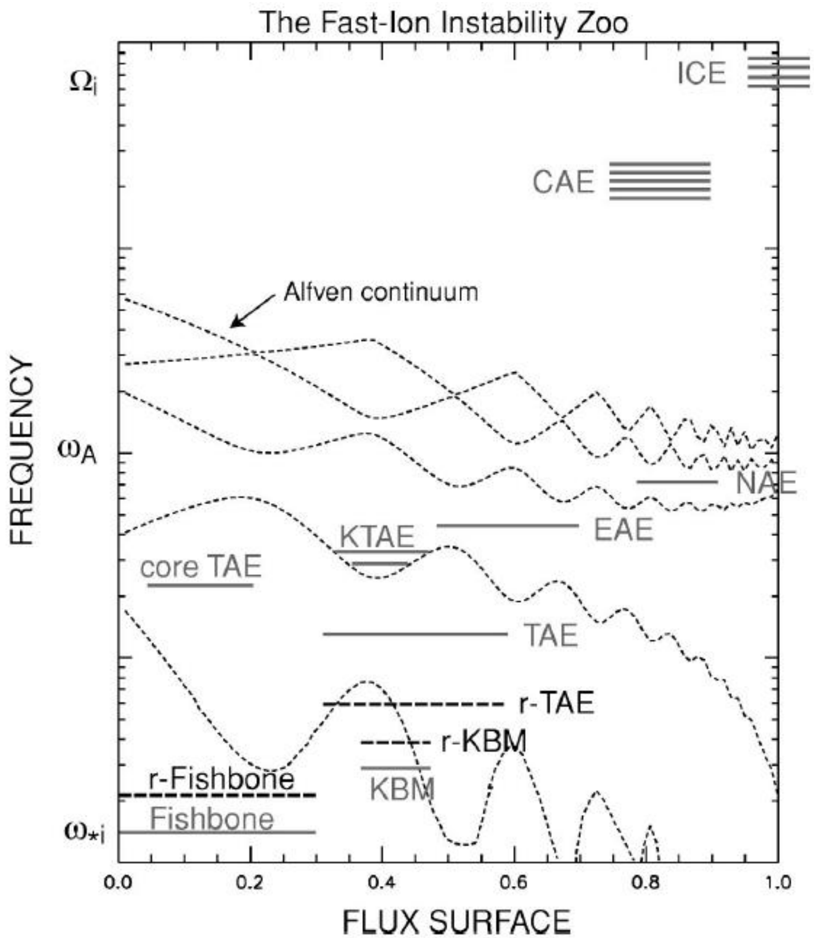

- **Fundamental freq. of observed instabilities lies between 1–10 MHz**

[1] Heidbrink PoP 2002

Compressional Alfvén eigenmodes are most likely candidates for observed instabilities

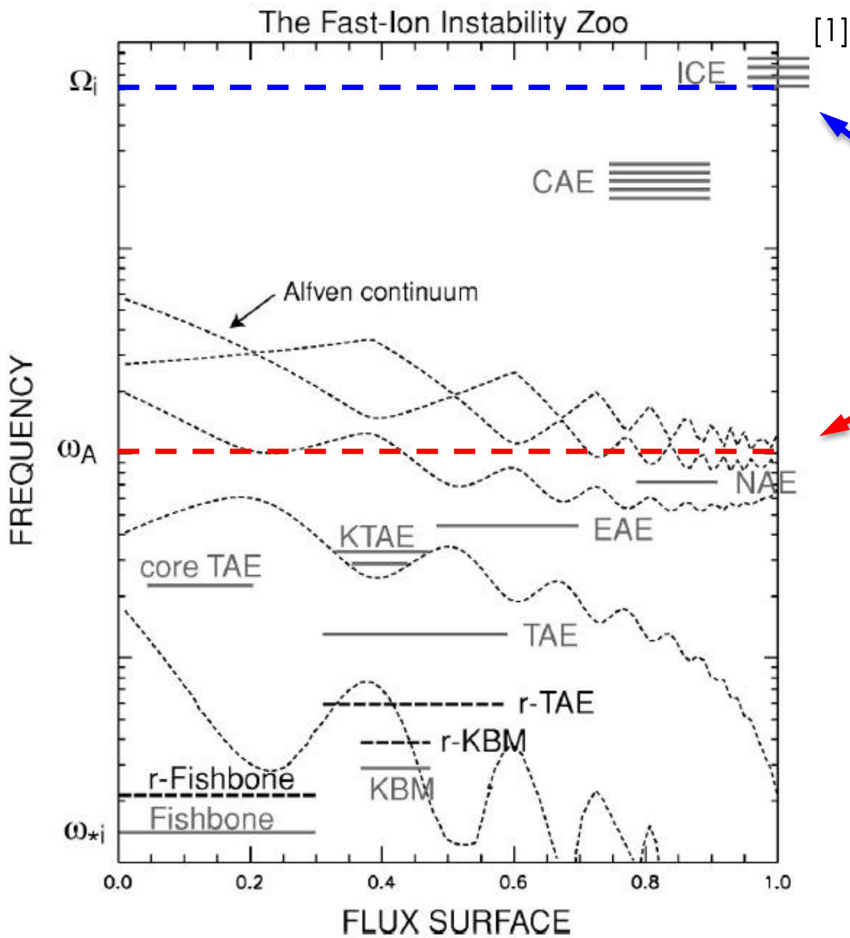

- **Fundamental freq. of observed instabilities lies between 1–10 MHz**
- **For given plasma parameters:**
  - $f_{ci} \approx 15$ MHz
  - $f_A \approx 1.5$ MHz

[1] Heidbrink PoP 2002

Compressional Alfvén eigenmodes are most likely candidates for observed instabilities

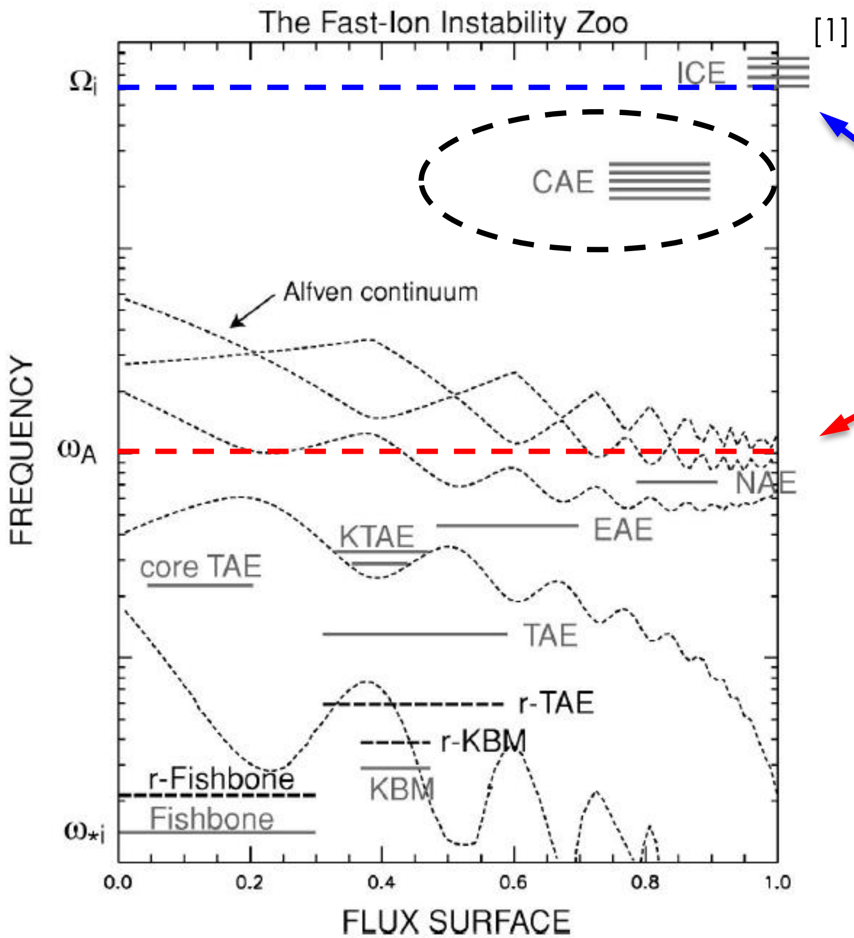

- **Fundamental freq. of observed instabilities lies between 1–10 MHz**
- **For given plasma parameters:**
  - $f_{ci} \approx 15$ MHz
  - $f_A \approx 1.5$ MHz
- **Compressional Alfvén eigenmodes (CAEs) are the most likely candidates for kinetic instabilities in the observed frequency region**

[1] Heidbrink PoP 2002

Compressional Alfvén eigenmodes are most likely candidates for observed instabilities

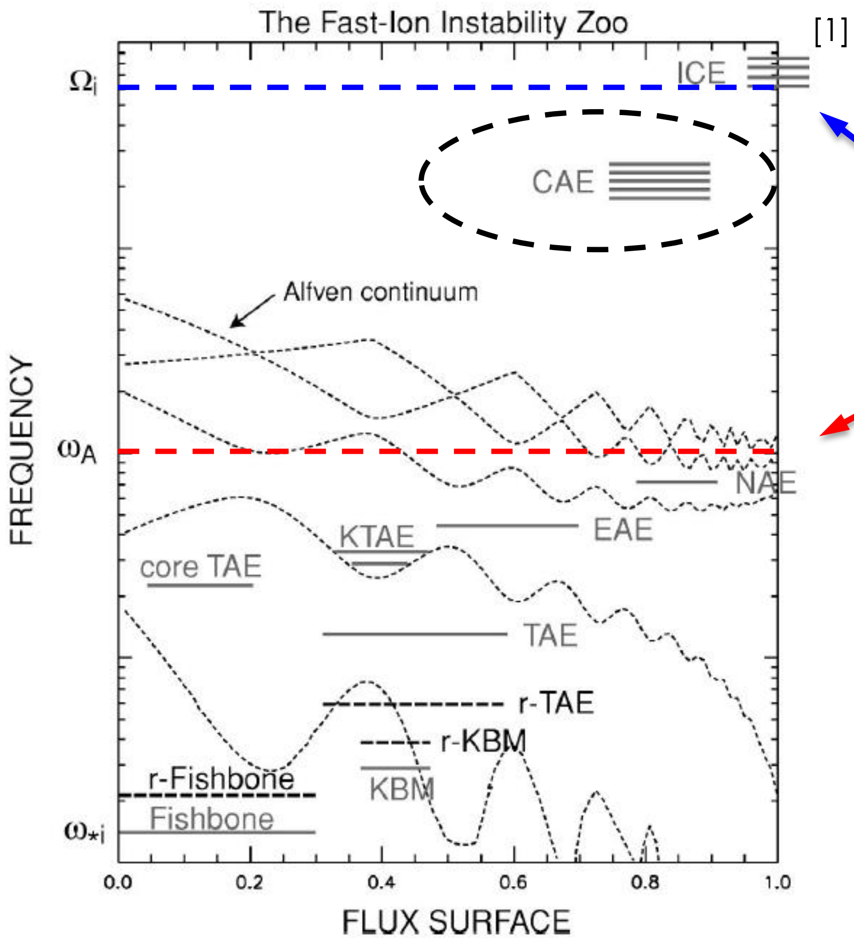

- **Fundamental freq. of observed instabilities lies between 1−10 MHz**
- **For given plasma parameters:**
  - $f_{ci} \approx 15$ MHz
  - $f_A \approx 1.5$ MHz
- **Compressional Alfvén eigenmodes (CAEs) are the most likely candidates for kinetic instabilities in the observed frequency region**
- Separate loops will be installed to measure toroidal numbers and polarization

See poster by Genevieve Degrandchamp on Thursday for details

[1] Heidbrink PoP 2002

Cherenkov resonance is a possible driving mechanism

- **Anomalous Doppler** and **Cherenkov resonances** are possible excitation mechanisms

$$\omega = k_{\parallel} V_{\parallel} - \frac{\omega_{ce}}{\gamma}$$

Satisfied at **large** $k_{\parallel}$ ($k_{\parallel} = 50\text{–}300\ m^{-1}$)

$$\omega = k_{\parallel} V_{\parallel}$$

Satisfied at **small** $k_{\parallel}$ ($k_{\parallel} = 0.1\text{–}2\ m^{-1}$)

Cherenkov resonance is a possible driving mechanism

- **Anomalous Doppler and Cherenkov resonances are possible excitation mechanisms**

$$\omega = k_{\parallel} V_{\parallel} - \frac{\omega_{ce}}{\gamma}$$

Satisfied at **large** $k_{\parallel}$ ($k_{\parallel}$ = 50–300 m^{-1})

$$\omega = k_{\parallel} V_{\parallel}$$

Satisfied at **small** $k_{\parallel}$ ($k_{\parallel}$ = 0.1–2 m^{-1})

- **Assume cold plasma dispersion relation at small $k_{\parallel} \approx k < 5$ m^{-1}**

$$\omega = kV_A\sqrt{1 + k_{\parallel}^2 c^2/\omega_{pi}^2}$$

Cherenkov resonance is a possible driving mechanism

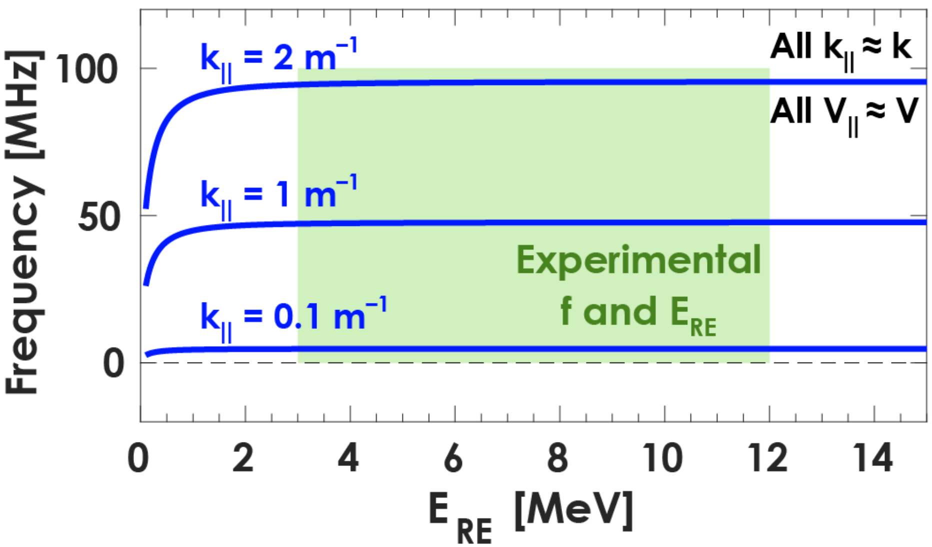

Cherenkov resonances at different $k_{||}$

- **Anomalous Doppler** and **Cherenkov resonances** are possible excitation mechanisms

$$\omega = k_{\|} V_{\|} - \frac{\omega_{ce}}{\gamma}$$

Satisfied at **large** $k_{||}$ ($k_{||}$ = 50−300 m^{-1})

$$\omega = k_{\|} V_{\|}$$

Satisfied at **small** $k_{||}$ ($k_{||}$ = 0.1−2 m^{-1})

- **Assume cold plasma dispersion relation at small $k_{||} \approx k < 5$ m^{-1}**

$$\omega = k V_A \sqrt{1 + k_{\|}^2 c^2 / \omega_{pi}^2}$$

- **Cherenkov resonance is satisfied for experimental conditions**

DIII-D NATIONAL FUSION FACILITY SAN DIEGO

Resonant RE orbits can be used to locate the RE bump

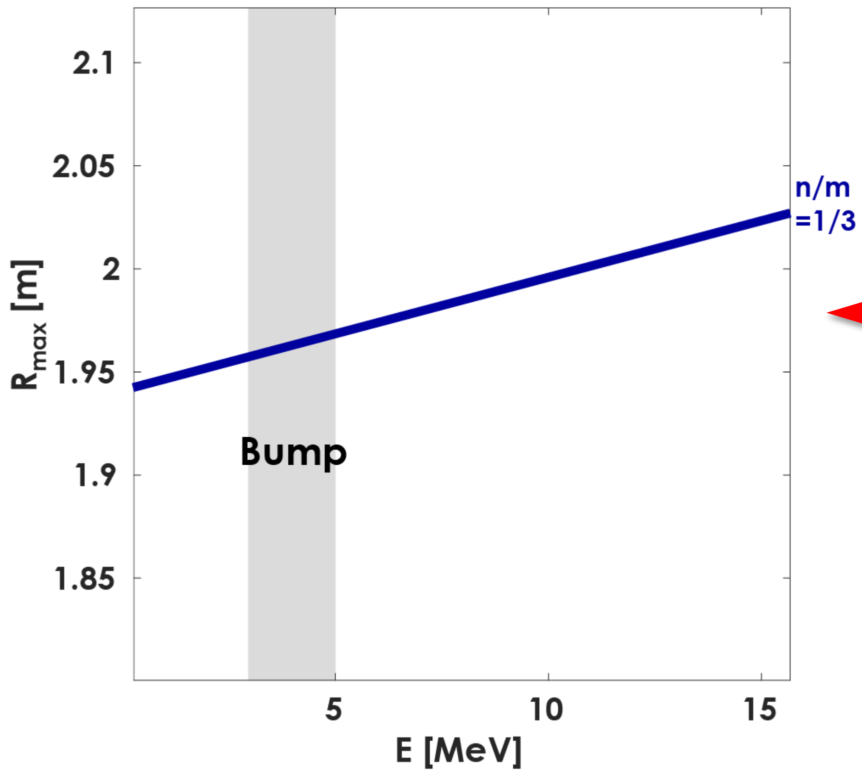

Example of n/m=1/3 resonant mode
Assumed: pitch-angle = −1 (WRT to current)
frequency = 3 MHz

- **Plasma equilibrium and RE orbits are calculated for the early stage of chirping instabilities**
- **Analysis of toroidal (ω_ϕ) and poloidal (ω_θ) transit frequencies provides wave-particle resonances:**

$$\Omega_{nm} = n\omega_\varphi - m\omega_\theta - \omega = 0$$

Resonant RE orbits can be used to locate the RE bump

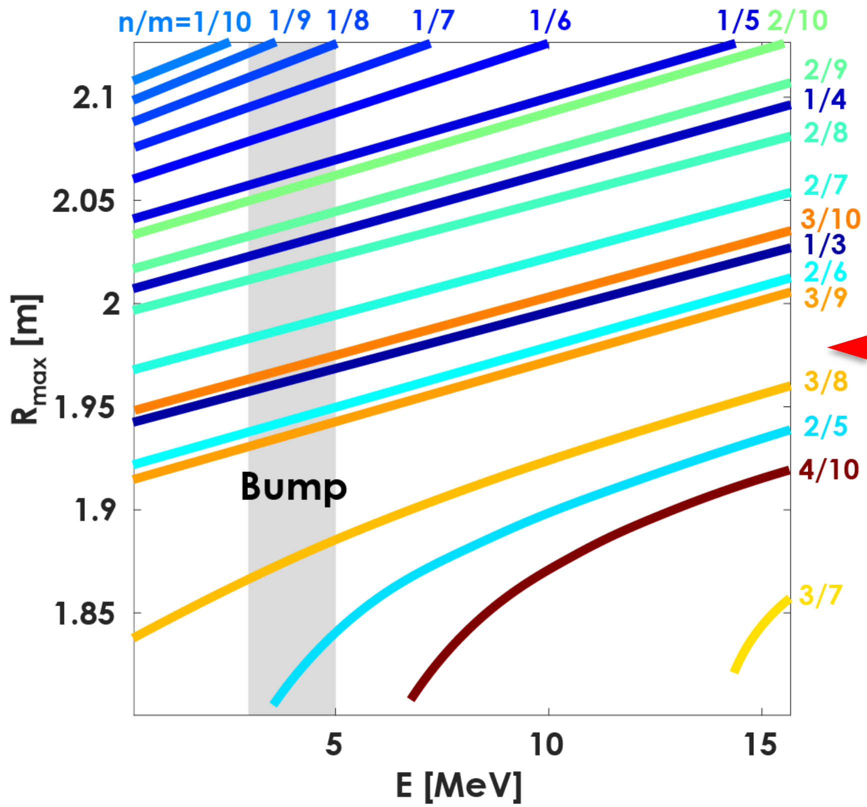

Example of resonant modes
for n = 0…4 and m = 0…10
Assumed: pitch-angle = −1 (WRT to current)
frequency = 3 MHz

- **Plasma equilibrium and RE orbits are calculated for the early stage of chirping instabilities**
- **Analysis of toroidal (ω_ϕ) and poloidal (ω_θ) transit frequencies provides wave-particle resonances:**

$$\Omega_{nm} = n\omega_\varphi - m\omega_\theta - \omega = 0$$

- **Calculations of RE loss on resonant orbits can be used for bump localization (modelling input is welcome!)**

DIII-D NATIONAL FUSION FACILITY SAN DIEGO

Outline

- Experiment and diagnostics
- Frequency chirping
- RE distribution function
- Operating space
- Possible driving mechanism and candidate instability
- RE-driven instabilities at higher collisionality

RE-driven MHz instabilities are also observed at high plasma collisionality

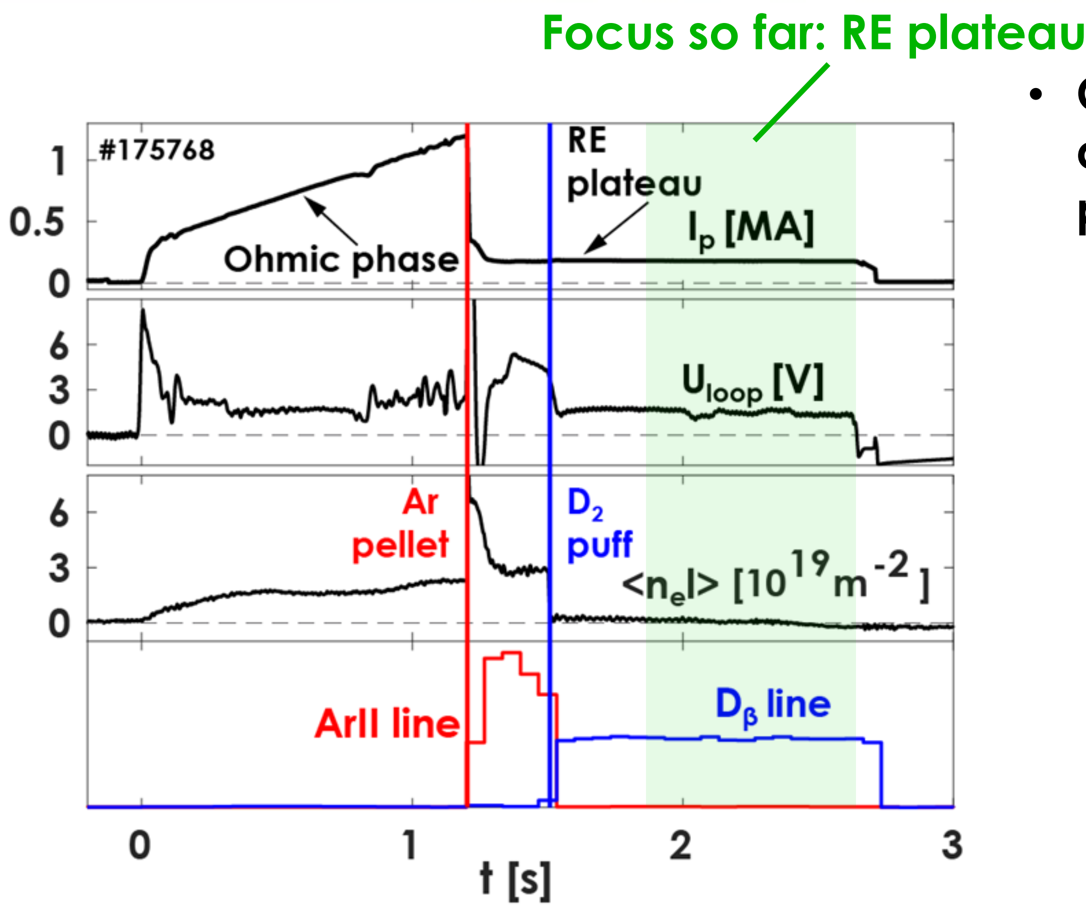

- **Chirping instabilities are accessed during the RE plateau at very low plasma density**

DIII-D NATIONAL FUSION FACILITY SAN DIEGO

RE-driven MHz instabilities are also observed at high plasma collisionality

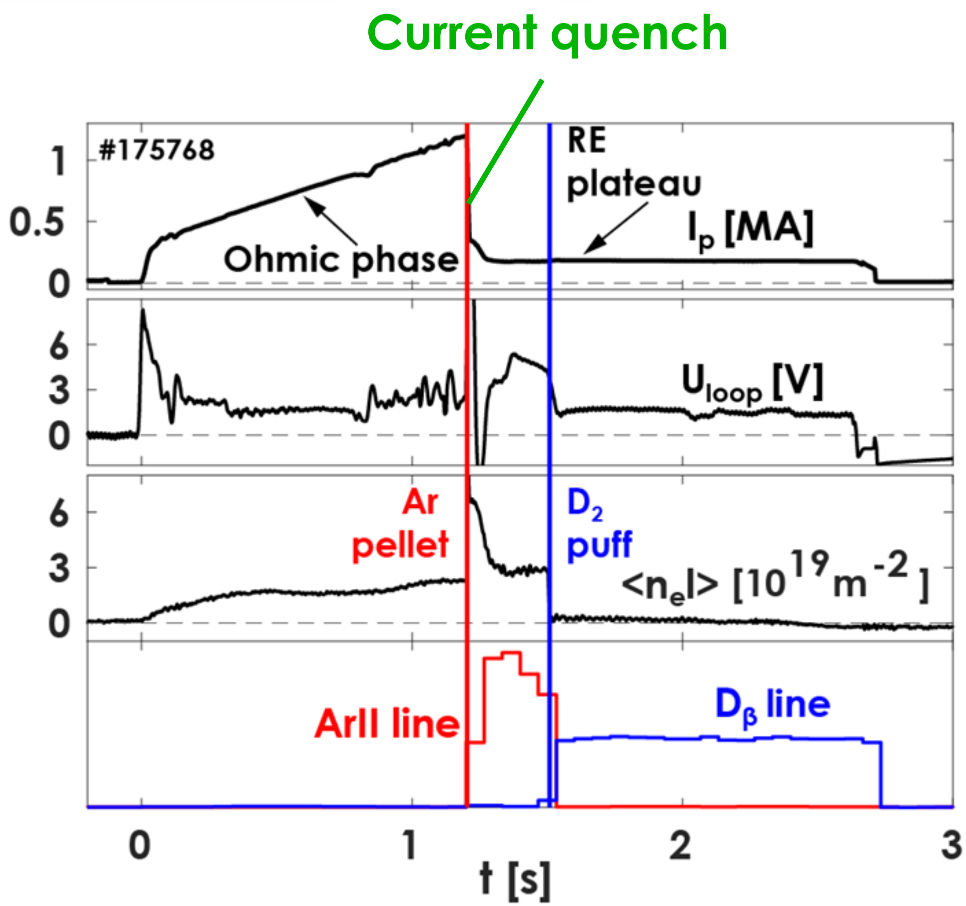

- **Chirping instabilities are accessed during the RE plateau at very low plasma density**

- **RE-driven instabilities are also detected right after impurity injection – during the current quench, when plasma is dense**
  - Most prominent after massive gas injection

DIII-D NATIONAL FUSION FACILITY SAN DIEGO

RE-driven MHz instabilities are also observed at high plasma collisionality

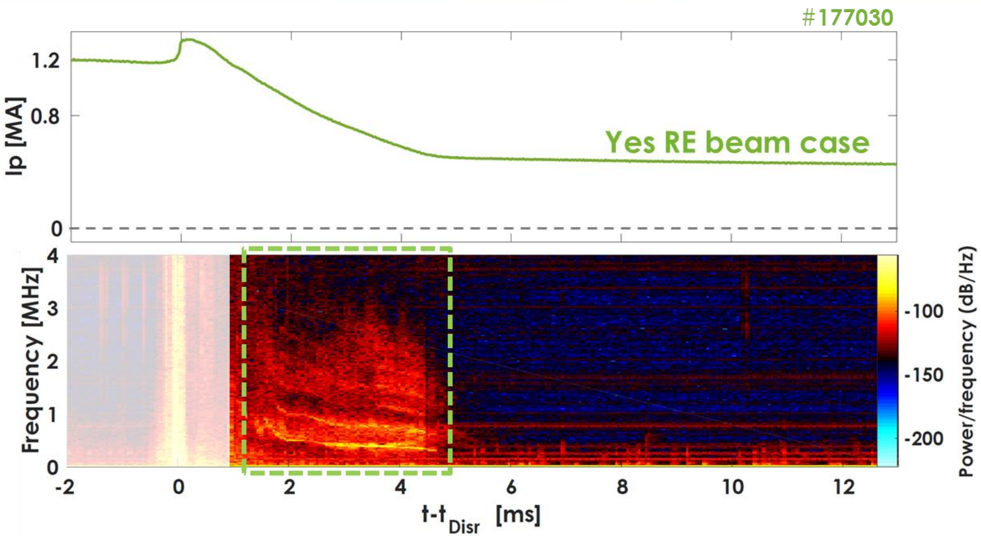

- **Chirping instabilities are accessed during the RE plateau at very low plasma density**
- **RE-driven instabilities are also detected right after impurity injection – during the current quench, when plasma is dense**
  - Most prominent after massive gas injection
- **These instabilities can be responsible for failure of RE beam formation**

RE-driven MHz instabilities are also observed at high plasma collisionality

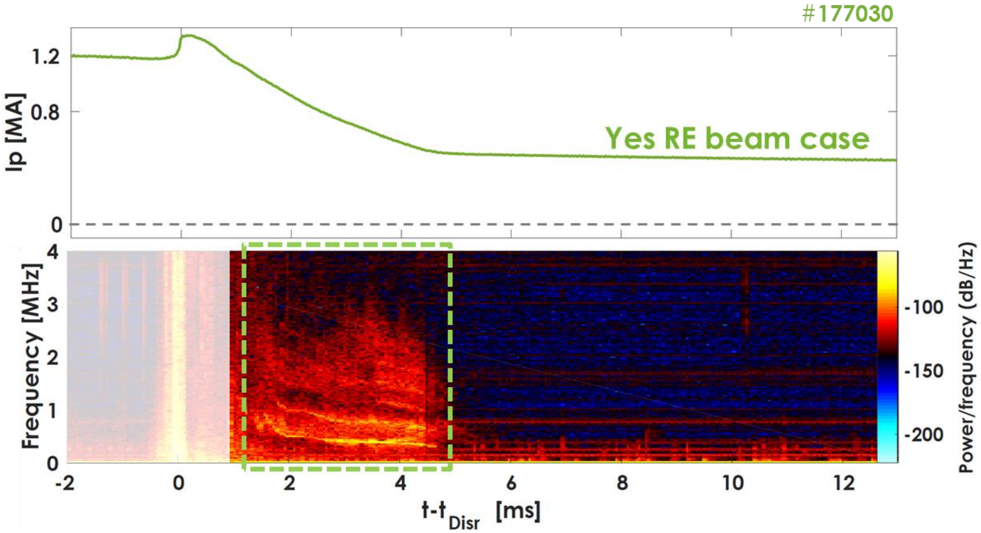

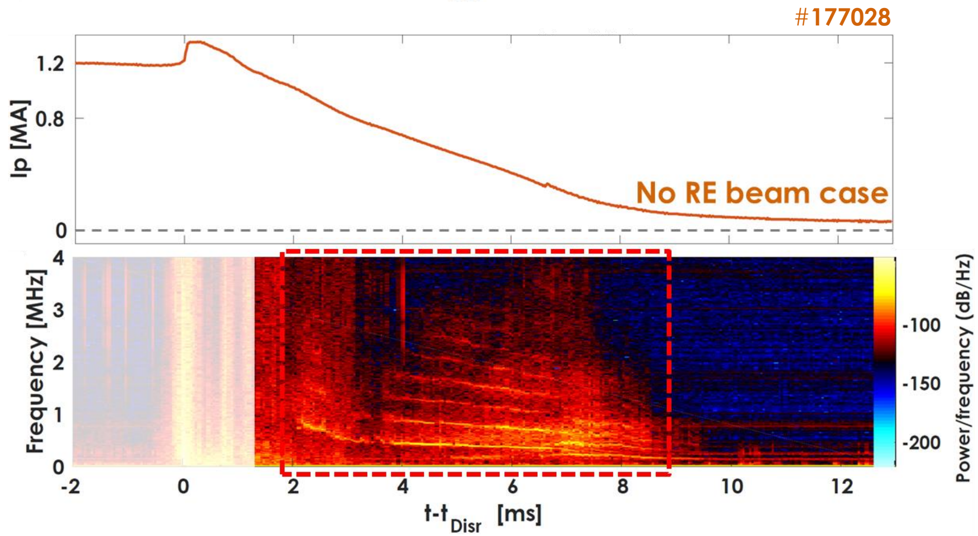

- **Chirping instabilities are accessed during the RE plateau at very low plasma density**
- **RE-driven instabilities are also detected right after impurity injection – during the current quench, when plasma is dense**
  - Most prominent after massive gas injection
- **These instabilities can be responsible for failure of RE beam formation**
- **Great interest for RE control in tokamaks!**

RE-driven instabilities observed during formation of post-disruption RE beam sometimes presumably kill it [1]

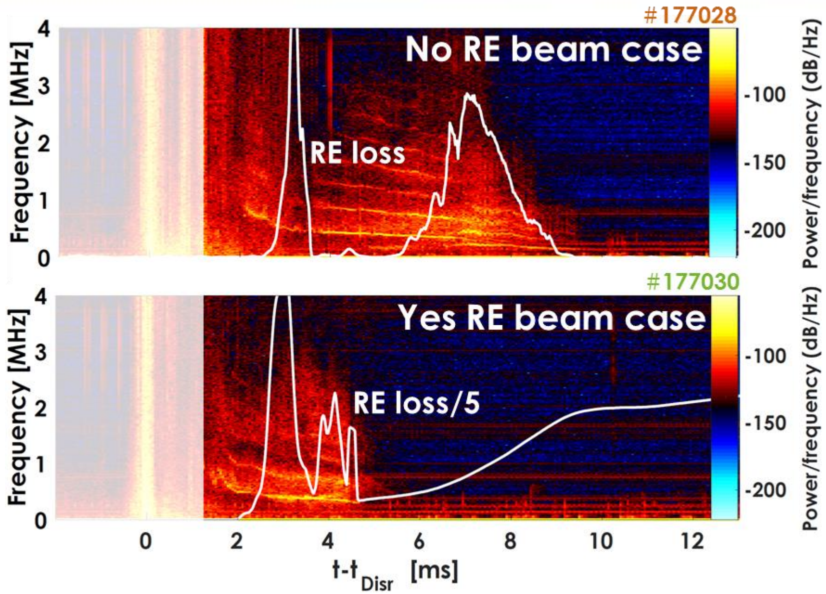

- **Disruptions without formation of RE beam show clear extended fluctuations of magnetic signals during the current quench**

- **RE loss correlates with MHz magnetic fluctuations in the frequency range of 0.1−3 MHz**

[1] See much more detail in Lvovskiy *et al.* PPCF 2018

RE-driven instabilities observed during formation of post-disruption RE beam sometimes presumably kill it [1]

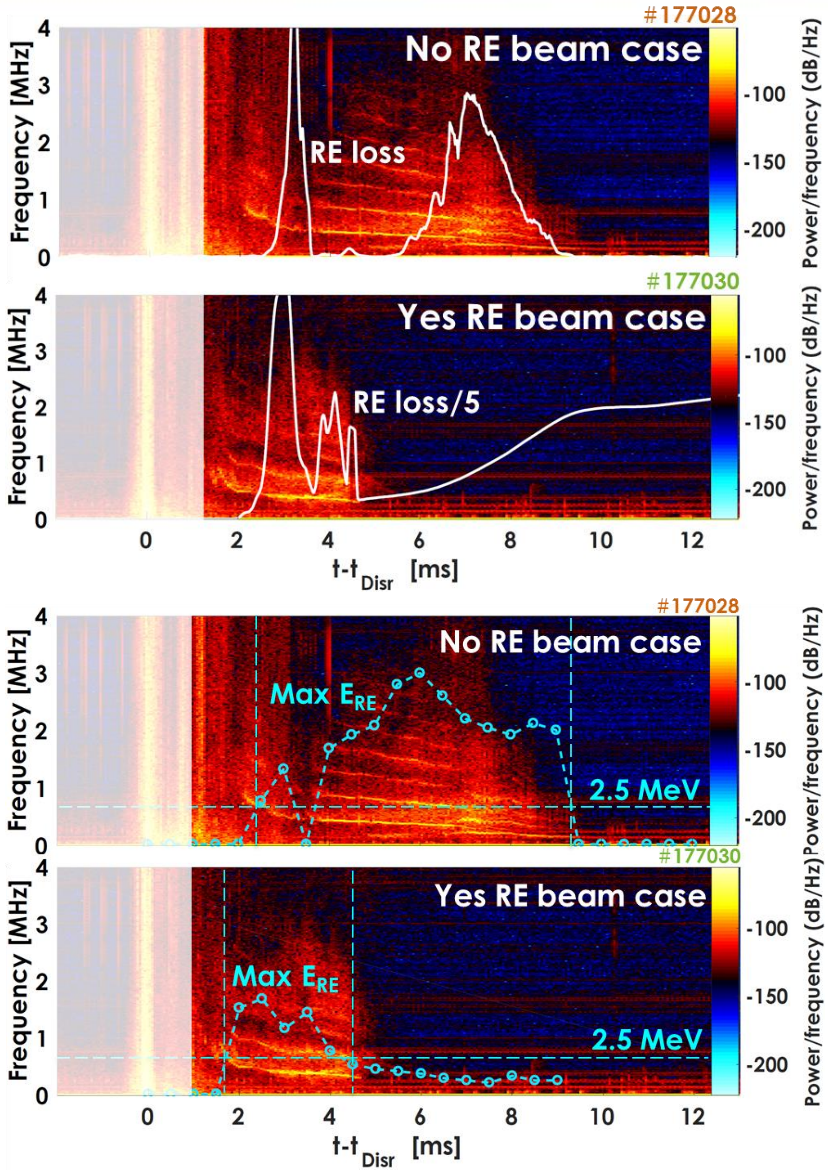

- **Disruptions without formation of RE beam show clear extended fluctuations of magnetic signals during the current quench**
- **RE loss correlates with MHz magnetic fluctuations in the frequency range of 0.1−3 MHz**
- **These magnetic fluctuations appear when RE energy E_{RE} exceeds 2.5–3 MeV**

[1] See much more detail in Lvovskiy *et al.* PPCF 2018

RE-driven instabilities observed during formation of post-disruption RE beam sometimes presumably kill it [1]

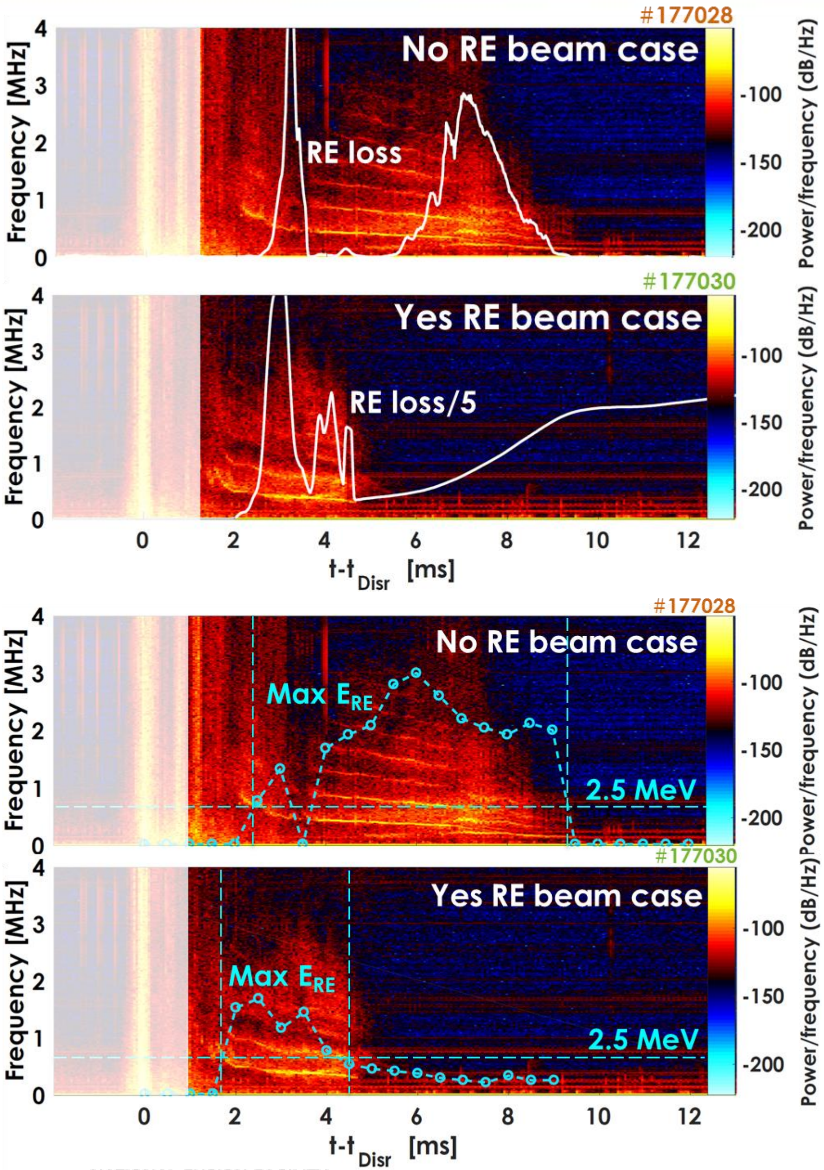

- **Disruptions without formation of RE beam show clear extended fluctuations of magnetic signals during the current quench**
- **RE loss correlates with MHz magnetic fluctuations in the frequency range of 0.1–3 MHz**
- **These magnetic fluctuations appear when RE energy E_{RE} exceeds 2.5–3 MeV**
- **Varying pre-disruption Ip and amount of injected Ar we can switch between cases w/ and w/o RE beam**

[1] See much more detail in Lvovskiy *et al.* PPCF 2018

CAEs can be excited by REs with bump-on-tail f(E) via Cherenkov resonance [1]

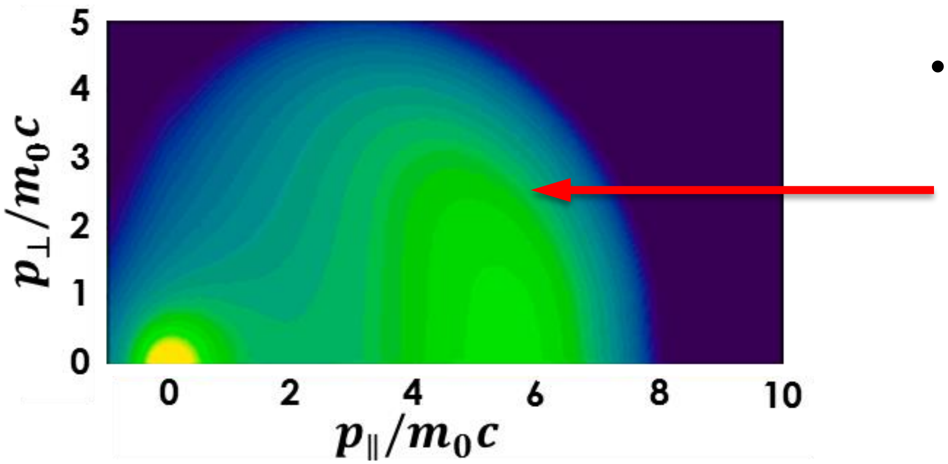

- Collisional and pitch-angle scattering of REs by argon nuclei can lead to formation of <u>RE distribution function with bump-on-tail</u> [2,3]

[1] Chang Liu *et al*. In preparation
[2] Hesslow *et al*. PRL 2017
[3] Chang Liu *et al*. PRL 2018

CAEs can be excited by REs with bump-on-tail f(E) via Cherenkov resonance [1]

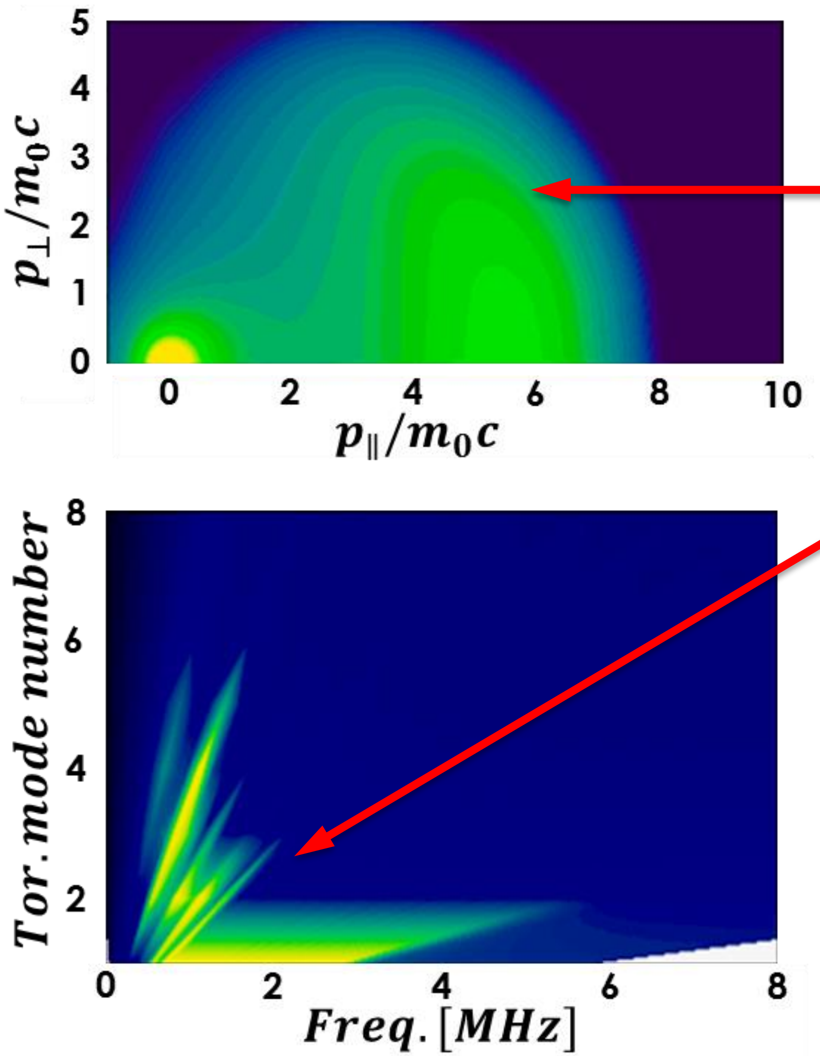

- **Collisional and pitch-angle scattering of REs by argon nuclei can lead to formation of <u>RE distribution function with bump-on-tail</u> [2,3]**
- **Quasilinear simulations show excitation of CAEs via Cherenkov resonance**

[1] Chang Liu *et al*. In preparation
[2] Hesslow *et al*. PRL 2017
[3] Chang Liu *et al*. PRL 2018

CAEs can be excited by REs with bump-on-tail f(E) via Cherenkov resonance [1]

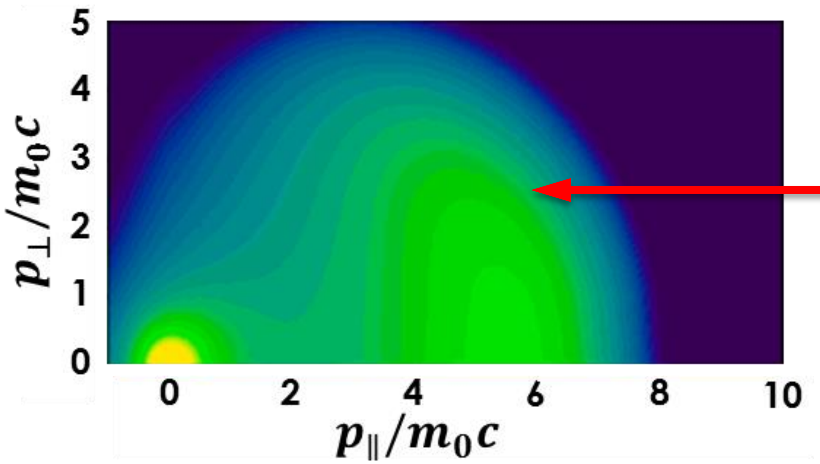

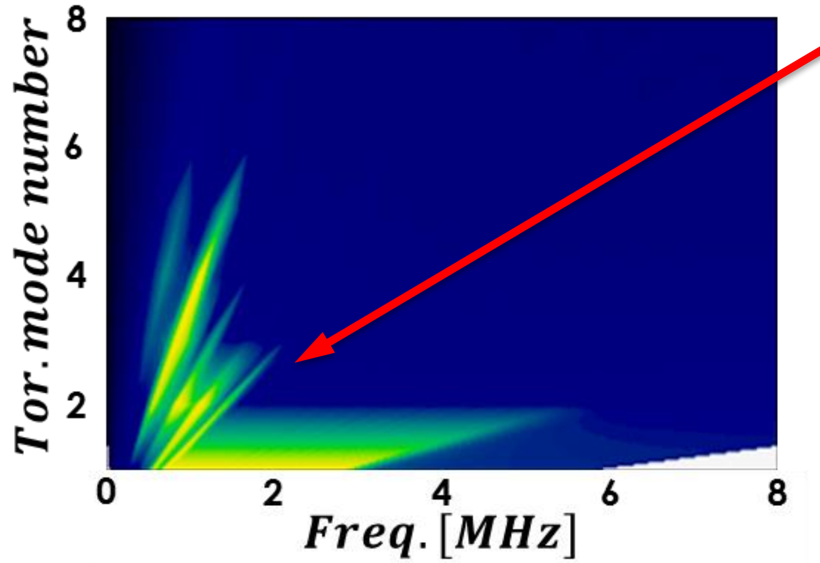

- Collisional and pitch-angle scattering of REs by argon nuclei can lead to formation of <u>RE distribution function with bump-on-tail</u> [2,3]
- Quasilinear simulations show excitation of CAEs via Cherenkov resonance
- Multiple modes can lead to stochastic motion of REs towards the wall
- This increases RE radial transport

[1] Chang Liu *et al*. In preparation
[2] Hesslow *et al*. PRL 2017
[3] Chang Liu *et al*. PRL 2018

RE-driven frequency chirping instabilities are observed for the first time in a tokamak

- **Instabilities are accessed in low density RE plateau under applied decelerating loop voltage**
- **Frequency chirps by 0.3−2.4 MHz on timescale of 1 ms**
- **There are two frequency regions: 1−10 MHz and 30−80 MHz**
  - Low-frequency instabilities correlate with increased RE loss
- **Modification of RE energy distribution function is measured during chirping in low-frequency region consistent with hole-clump model**
- **Candidate modes are CAEs driven by non-monotonic RE distribution function via Cherenkov resonance**
- **Similar frequency instabilities correlated with intermittent RE loss are also observed at high plasma collisionality – during current quench**
  - They are presumably responsible for non-sustainable RE beam
  - Modelling shows excitation of CAEs and increased RE radial transport

(Highlight slide) Rapid frequency chirping instabilities driven by runaway electrons are observed for the first time in a tokamak

- **Instabilities are accessed in low density post-disruption runaway plasma under applied decelerating voltage in DIII-D**
- **Frequency chirps by 0.3–2.4 MHz on timescale of 1 ms**
- **There are two distinct frequency regions: 1–10 MHz and 30–80 MHz**
  - Low-frequency instabilities correlate with intermittent RE loss
- **Modification of RE energy distribution function is measured during chirping in low-frequency region consistent with hole-clump model**

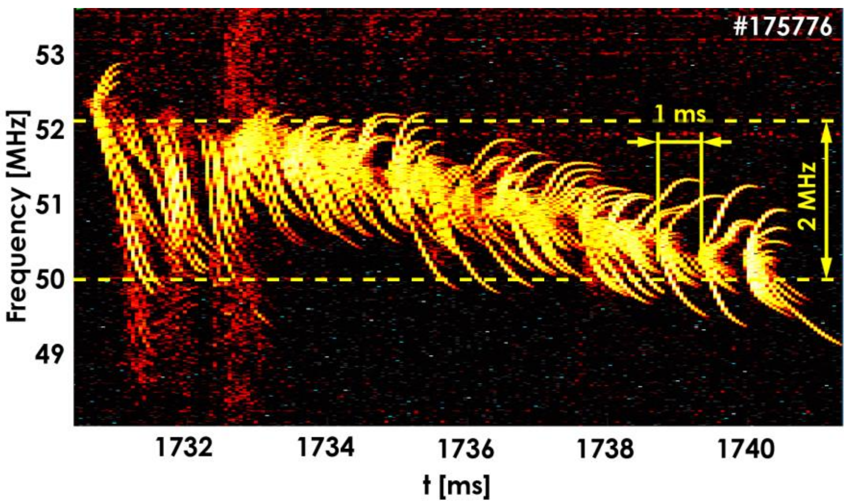

Magnetic spectrogram of frequency chirping instabilities driven by runaway electrons in DIII-D

Lvovskiy *et al*. *Observation of rapid frequency chirping instabilities driven by runaway electrons in a tokamak.* Submitted to Nucl. Fusion

BONUS SLIDES

Approximate phase space sensitivity of RE diagnostics

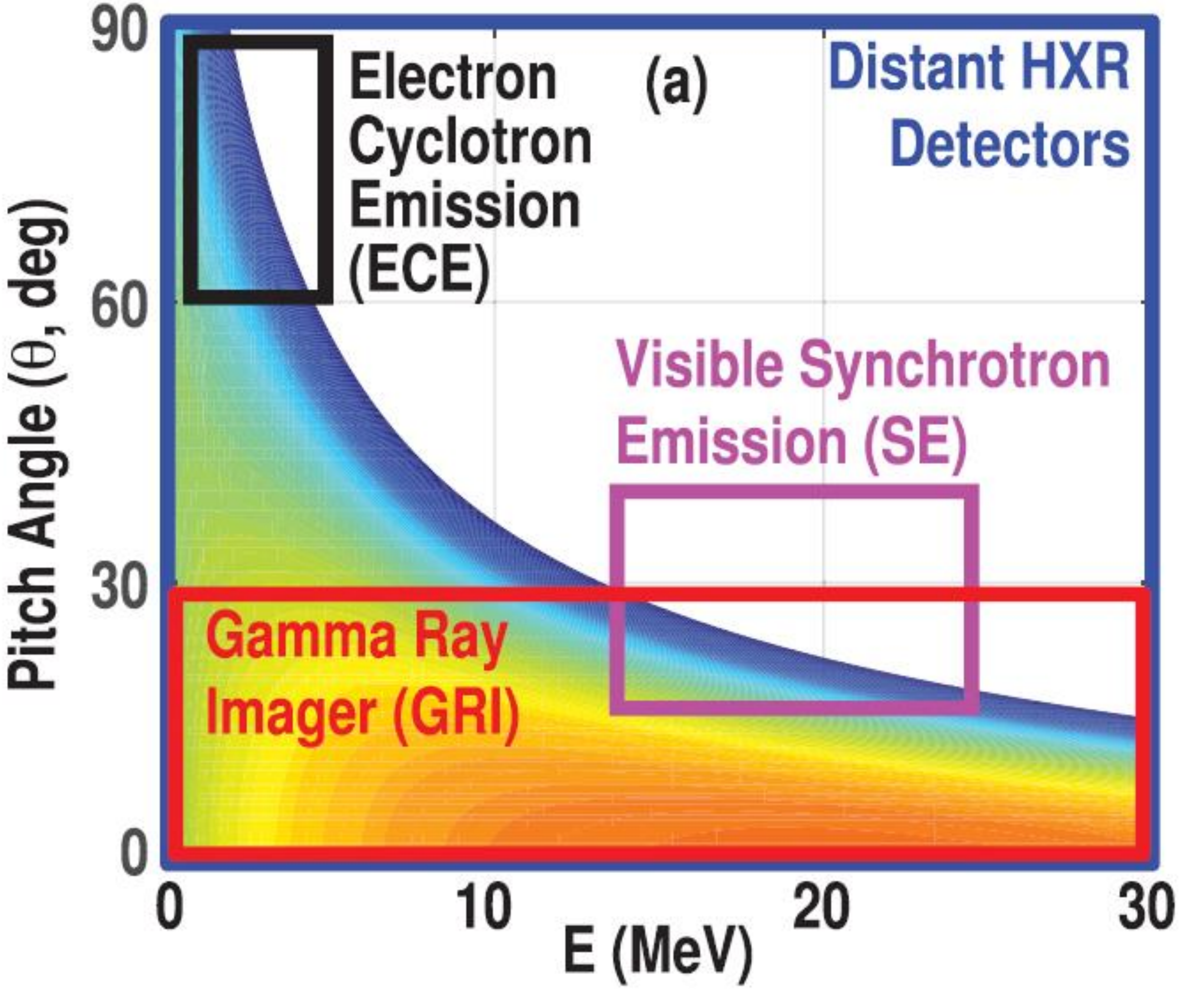

Paz-Soldan *et al*. PoP 2018

Backup: RE spectrum is reconstructed from HXR spectrum using onion-peel method

- **Onion peel method from high energy down can be used to go from HXR to electron spectrum**
  - Zero pitch angle and spatial homogeneity are assumed

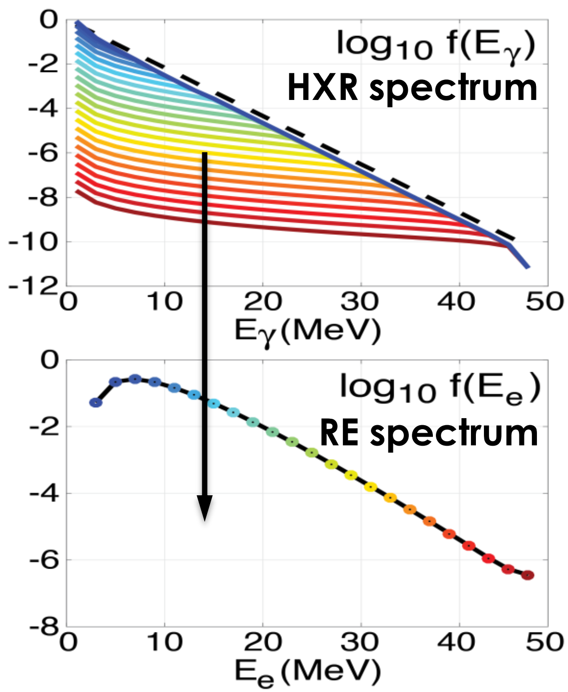

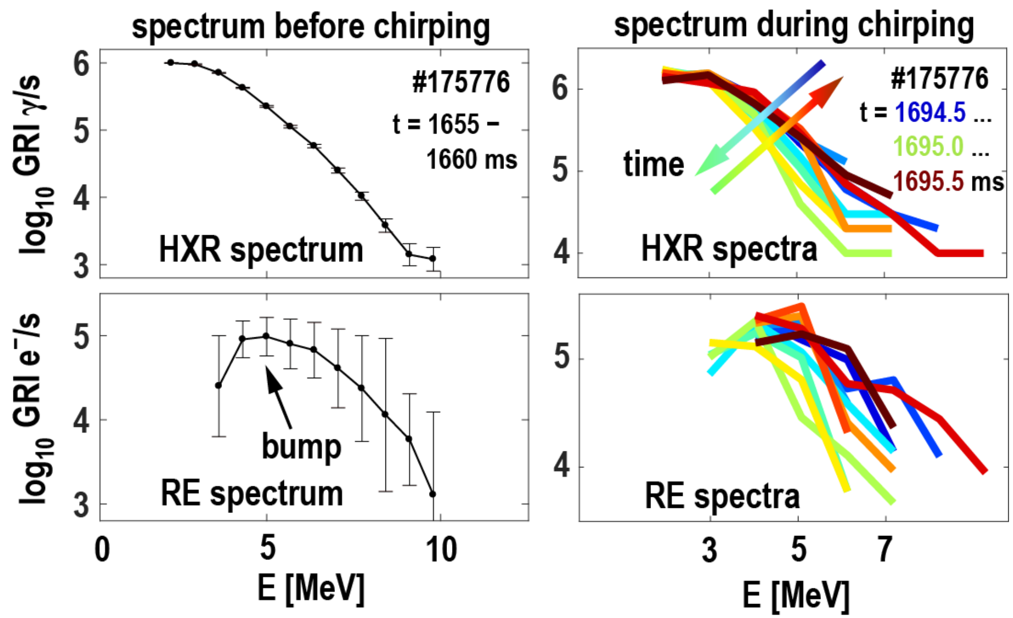

HXR and RE spectra in the experiment

Backup: DIII-D gamma ray imager (GRI) provides 2D view of RE bremsstrahlung emission

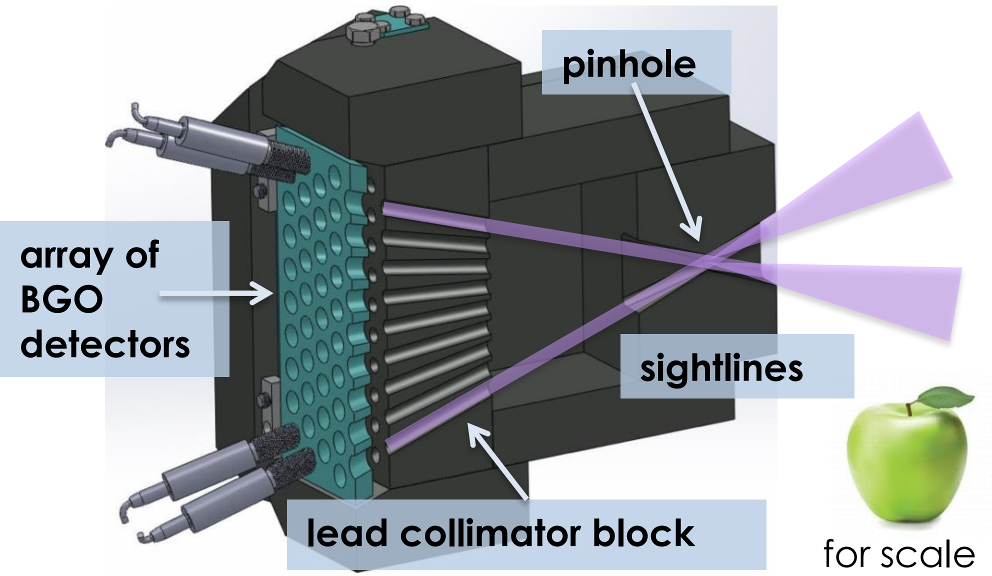

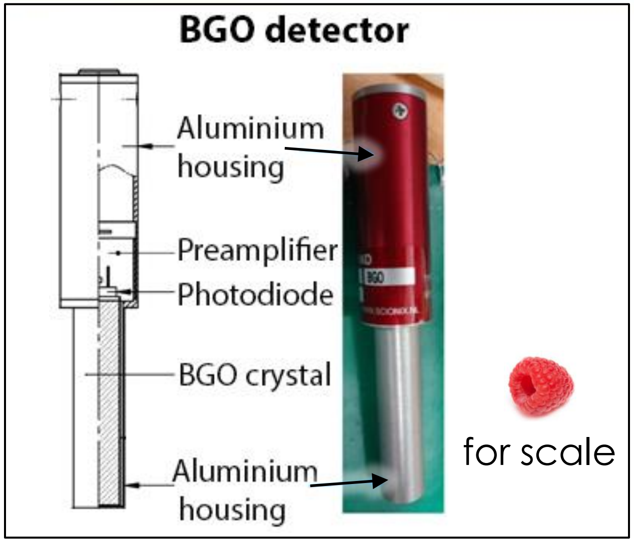

- GRI is a pinhole camera
- Its array consists of gamma scintillator detectors (up to 123 places)
- Body and collimator block are made of lead (≈ 190 kg)

[Pace et al. RSI 2016]

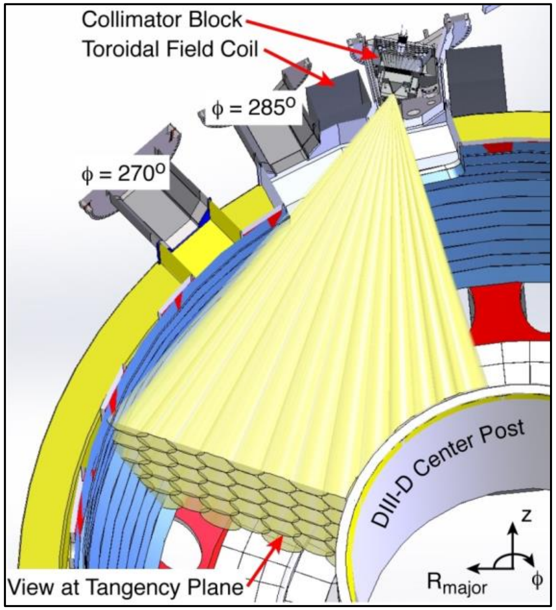

DIII-D toroidal cross-section

Backup: Bremsstrahlung spectra can be found using pulse height analysis. Example: QRE shot

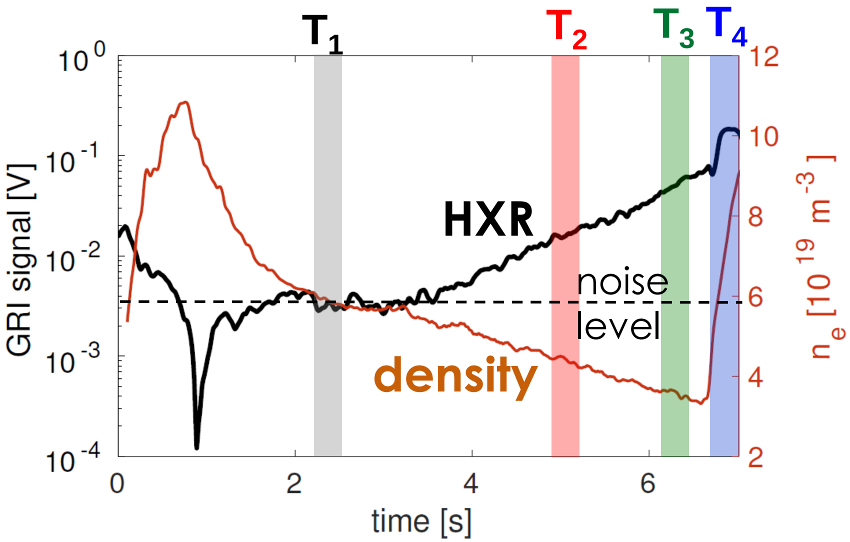

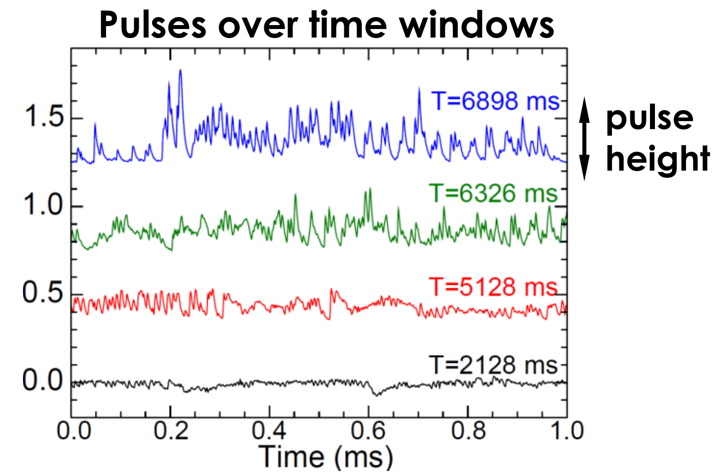

- Time traces are comprised of pulses from distinct gamma particles
- Gamma particles are analyzed via pulse height analysis (PHA)
- Bremsstrahlung spectrum hardens in the course of time

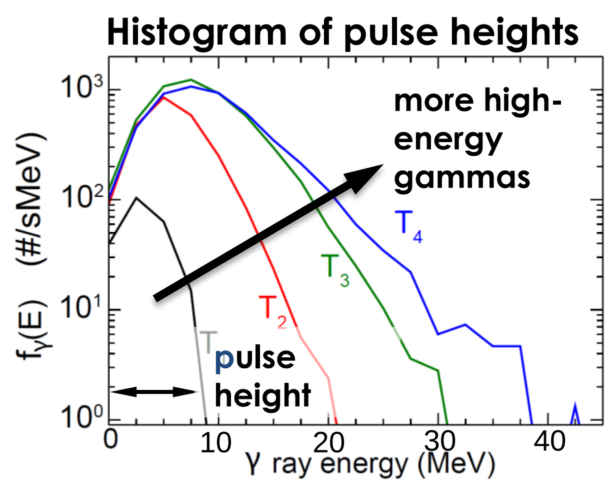

[Cooper et al. RSI 2016]

Backup: Measurements during the RE plateau regime are challenging – upgrade with fast gamma detectors

- **Gamma flux due to bremsstrahlung emission is higher by 10^3–10^4 in RE plateau regime compared to QRE**
- **BGO detectors are usually saturated after the disruption**
- **New LYSO+MPPC detectors are capable to measure during the post-disruption stage**

Collaboration with U. Milano-Bicocca

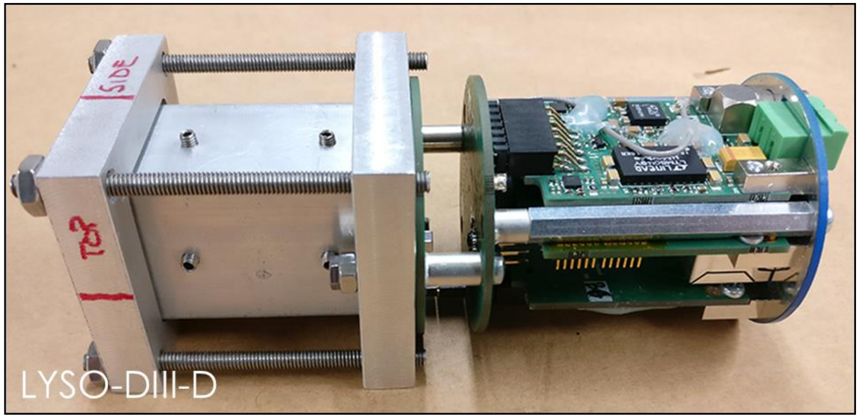

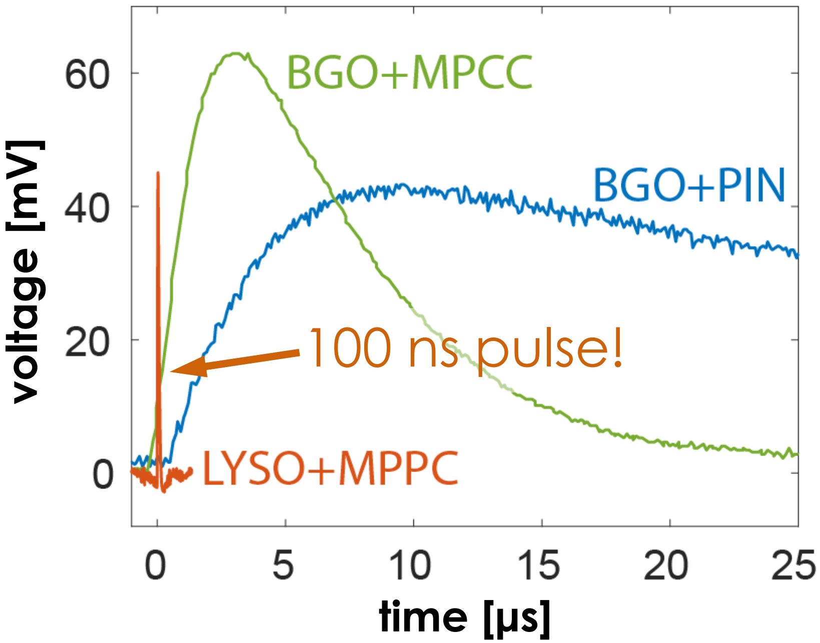

Response of gamma detectors to a single gamma pulse

Backup: Frequency dependence on n_e is stronger than Alfvénic

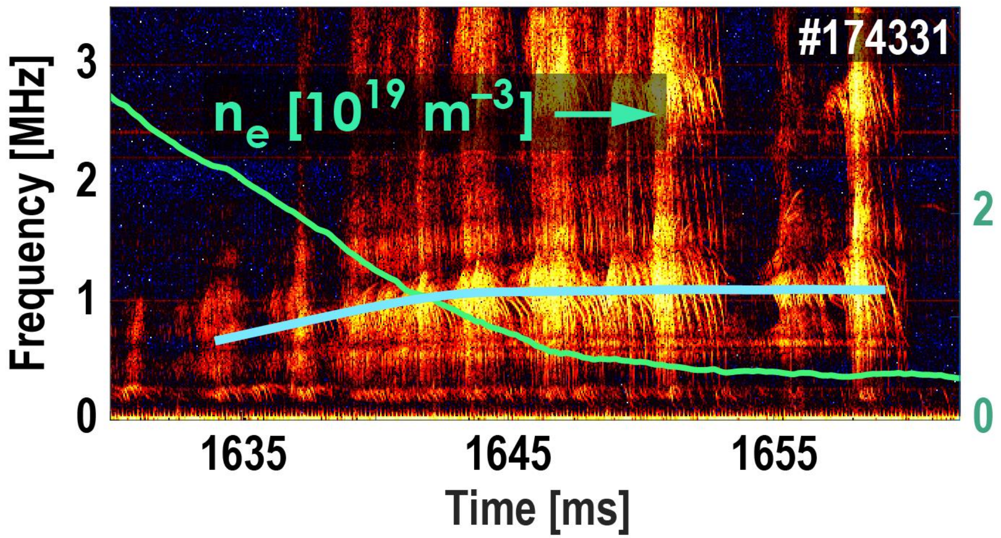

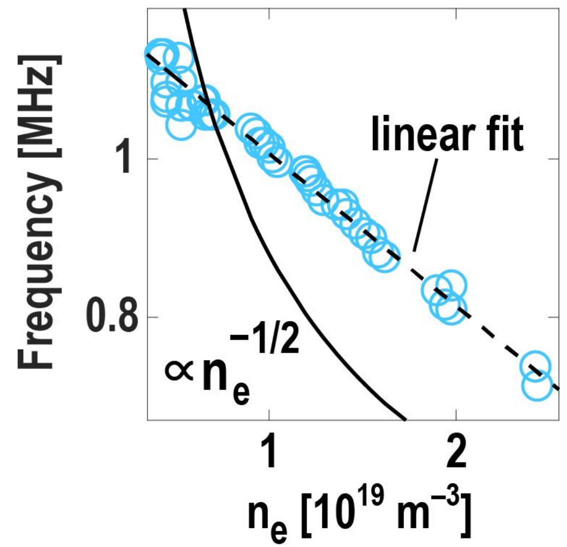

- Frequency decreases as n_e^{-1} while typical Alfvénic dependence is $n_e^{-1/2}$
- Possibly explained by plasma non-uniformity during the argon purge

Backup: More energetic RE distribution leads to no RE beam

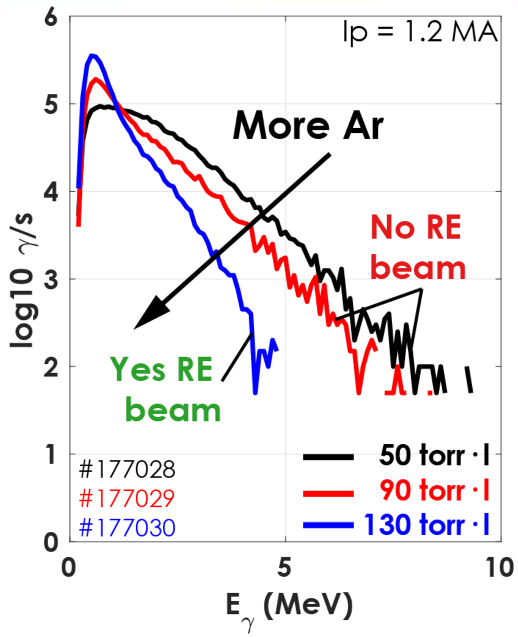

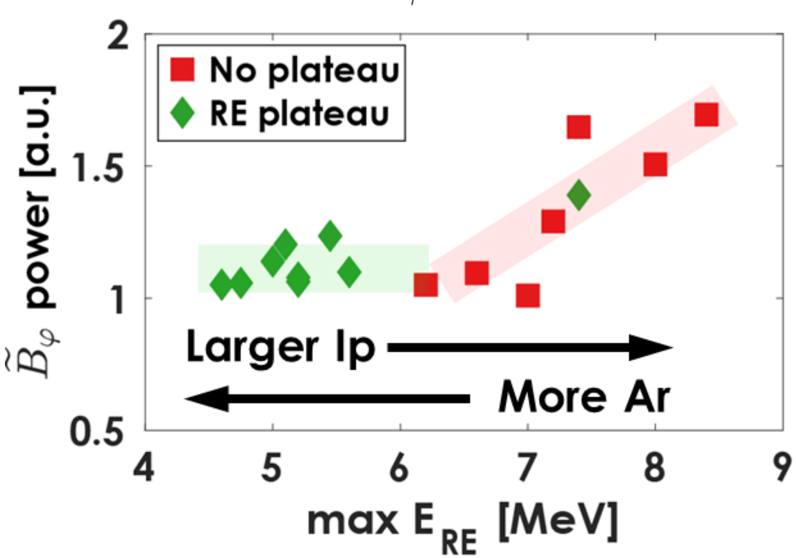

- Cases without RE beam correlate with more energetic RE distribution
- Increased argon quantity reduces the number of high-energy REs and correlates with successful RE beam formation
- Integrated power of MHz frequency magnetic signals increases with increase of max E_{RE}
- Increased pre-disruption plasma current increases the maximum energy of REs

Backup: Possible mechanism of suppression of RE beam formation with two actuators

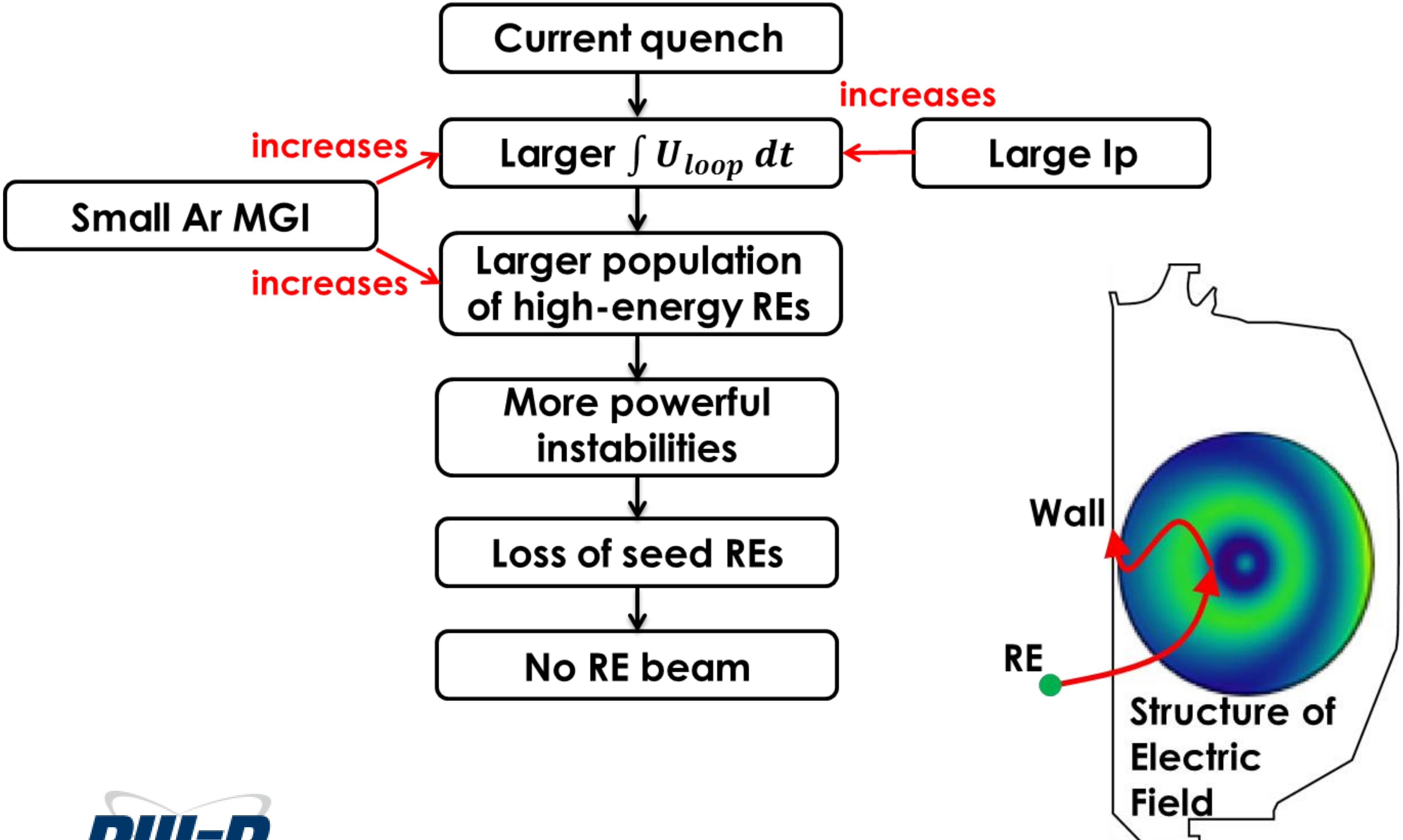

DIII-D NATIONAL FUSION FACILITY SAN DIEGO